



ELSEVIER

Journal of Volcanology and Geothermal Research 117 (2002) 169–194

Journal of volcanology
and geothermal research

www.elsevier.com/locate/jvolgeores

Petrology and geochemistry of the 1991 and 1998–1999 lava flows from Volcán de Colima, México: implications for the end of the current eruptive cycle

James F. Luhr*

Department of Mineral Sciences, NHB-119, Smithsonian Institution, Washington, DC 20560, USA

Received 14 November 2000; accepted 24 August 2001

Abstract

Point-counted modes, representative mineral analyses, and whole-rock major- and trace-element compositions determined by X-ray fluorescence spectroscopy and inductively coupled plasma mass spectroscopy (ICP-MS) are presented for 11 samples of the hornblende–andesite block-lava flows erupted from Volcán de Colima in 1991 and 1998–1999. New ICP-MS trace-element data are also presented for 37 andesites erupted between 1869 and 1982, described in previous publications. These data are used to evaluate mineralogical and whole-rock compositional changes during two well-defined historical eruption cycles: 1818–1913 and 1913–present. The eruptive cycles of Volcán de Colima are dominated by andesitic lavas with ~ 61 wt% SiO_2 , but terminate with major explosive eruptions, as occurred in 1818 and 1913, involving relatively mafic andesites with ~ 58 % SiO_2 . Following eruptions of andesitic block-lava flows with ~ 61 % SiO_2 in 1961–1962 and 1975–1976, a trend toward lower SiO_2 contents began in 1976 and peaked in 1981, probably as a small volume of deeper, more mafic magma ascended into the shallower andesitic reservoir beneath the volcano. Since then, however, andesitic lavas have become progressively richer in SiO_2 through the 1991 and 1998–1999 eruptions. Andesites erupted between 1961 and 1999 show many subtle but important differences compared to those erupted between 1869 and 1913. Based on rocks of similar SiO_2 content, the 1961–1999 andesites are richer in modal plagioclase and in the elements Y, Nb, Tb, Ho, Er, Yb, and Ta, and they are poorer in modal hornblende and in the elements Ba and Sr. All of these observations are consistent with the interpretation that the magmas of 1961–1999 had significantly lower water contents compared to those erupted in 1869–1913, which diminished the role of hornblende crystallization and enhanced the role of plagioclase crystallization. The relatively lower magmatic water contents for the 1961–1999 andesites imply that the explosive eruption anticipated to terminate the current eruptive cycle will be less powerful than the 1913 eruption. Of equal importance to this question, however, is the role of magmatic degassing. The relatively higher viscosities of andesitic magmas with ~ 61 % SiO_2 likely lead to relatively slow ascent rates and more thorough degassing prior to arrival of the magma at the summit crater and its eruption as block lava. In contrast, the lower viscosities of more mafic andesitic magmas with ~ 58 % SiO_2 result in faster ascent and greater retention of volatiles, so that they erupt explosively upon reaching the summit crater. Published by Elsevier Science B.V.

Keywords: Volcán de Colima; pyroclastic flows; petrology; geochemistry

* Tel.: +1 (202) 357 4809; Fax: +1 (202) 357 2476. E-mail address: luhr@volcano.si.edu (J.F. Luhr).

1. Introduction

Monitoring of volcanic eruptions involves an ever-growing arsenal of methodologies. Although the founding disciplines of observational volcanology, gas/water geochemistry, and seismology still play critical roles, recent years have seen expanding applications of ground-deformation, microgravity, gas-phase spectroscopy, aircraft gas sampling, satellite-borne thermal, gas-species, and particle detection, and many other approaches (e.g. Scarpa and Tilling, 1996). Complementary petrological monitoring tools have also been utilized for study of sequentially erupted materials: lava, scoria, pumice, and ash. These petrologic approaches are themselves quite diverse and designed to address a variety of phenomena: (1) compositional studies of glass inclusions trapped in phenocrysts, which provide insight into pre-eruptive melt compositions, primary volatile contents, and magmatic degassing histories (e.g. Harris and Anderson, 1983; Métrich and Clocchiatti, 1989; Métrich et al., 1993; Ihinger et al., 1994); (2) measurements of reaction-rim widths on hornblende crystals, which can be related to magmatic ascent rates (Rutherford and Hill, 1993; Rutherford and Devine, 1998); (3) investigations of groundmass textures and phase compositions and their relationships to nucleation rates, crystal-growth rates, degassing events, and cooling histories (Cashman, 1988, 1992; Geschwind and Rutherford, 1995; Martel et al., 2000); and (4) investigations of mineralogical and whole-rock compositional changes during historical eruptions. The present study is of this type.

Whole-rock compositional changes have been interpreted to reflect a wide range of magmatic processes operating over a variety of time intervals. These include changes in mantle source regions and percentages of partial melting, different degrees of interaction with crustal rocks during ascent, and the likely operative processes in crustal magma reservoirs: fractional crystallization, magma mingling or mixing, wall-rock assimilation, and mafic magma influx (Wilcox, 1954; Cashman and Taggart, 1983; Melson, 1983; Camus et al., 1987; McBirney et al., 1987; Reagan et al., 1987; Luhr and Carmichael, 1990a; Fedotov

et al., 1991; Pallister et al., 1992, 1996; Corsaro and Cristofolini, 1996; Gamble et al., 1999; Hobden et al., 1999; Pietruszka and Garcia, 1999; Martel et al., 2000). Petrological studies of modern eruptions gain added importance when processes identified through study of erupted material can be related to signals recorded by seismic, geodetic, and other monitoring techniques (e.g. Pallister et al., 1996).

In order for a volcano to be a suitable candidate for whole-rock compositional monitoring of historical eruptions it must satisfy two criteria. It must erupt frequently, and have a long historical record. Volcán de Colima has had frequent eruptions extending back to the earliest reports during 1519–1523 (Bretón et al., 2002-this volume). Understandably, the quality of eruption reporting for the early part of this ~480-yr historical record is relatively poor, but new details emerge with each scholarly investigation, most recently Bretón et al. (2002-this volume). As reviewed below, Luhr and Carmichael (1980) proposed that the second half of the historical eruptive record of Volcán de Colima has been dominated by two similar cycles of activity, each lasting about a century: 1818–1913 and 1913–present (Fig. 1).

The transitions between these eruptive cycles, in 1818 and 1913, were marked by major explosive eruptions. No samples have yet been confidently identified from the 1818 event, but the 1913 scoriae are considerably more mafic than the andesitic block lavas erupted during intervening years (Luhr and Carmichael, 1980, 1990a). Assuming that the behavioral patterns of the past several centuries will persist, the present eruptive cycle should end in another major explosive eruption, like those in 1818 and 1913. This study was designed to evaluate the petrology and geochemistry of the lavas erupted in 1991 and 1998–1999 for insight into a transition to more mafic compositions, begun in 1976, that might herald the next major explosive eruption. In addition to major- and trace-element analyses by X-ray fluorescence (XRF) spectroscopy for 11 lava samples from the 1991 and 1998–1999 eruptions, new trace element data by inductively coupled plasma mass spectrometry (ICP-MS) are presented for those 11 samples plus an additional 37 samples from ear-

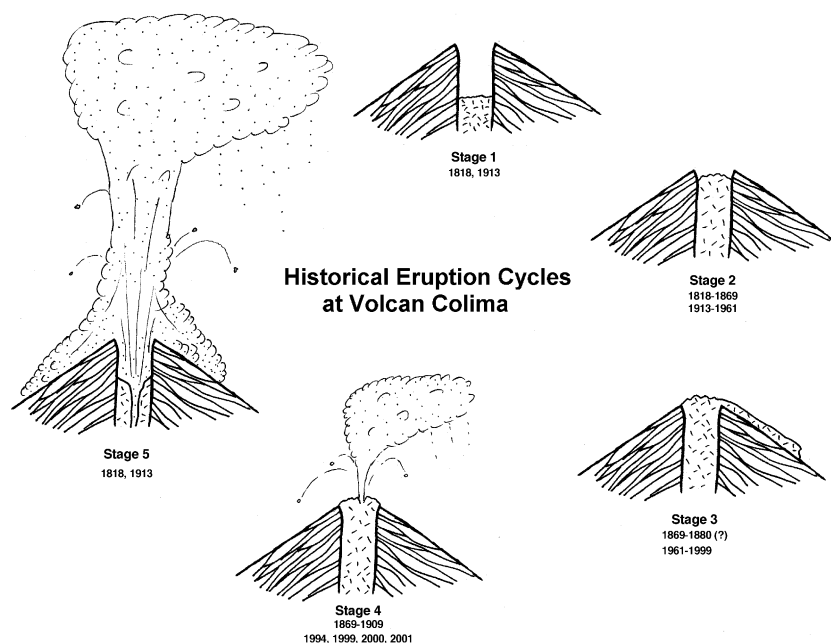


Fig. 1. Schematic depiction of five major stages in the last two historical eruption cycles of Volcán de Colima. Stage 1: Open crater following cycle-ending explosive eruptions. Stage 2: Lava dome slowly ascends in open crater, probably through a combination of endogenous growth and extrusions onto the crater floor. Stage 3: Crater dome reaches the rim (or magma leaks out a flank vent as in 1869) and block lava flows down the upper flanks of the cone, sometimes reaching 3–4 km distance. Block-and-ash flows precede and accompany emplacement of lava flows. Stage 4: Intermittent minor-to-major explosive activity (VEI 2–4) from the summit crater (or parasitic vent as in 1869) alternates with the stage-3 lava emissions. Stage 5: Major explosive eruptions (VEI ~4; Simkin and Siebert, 1994) terminate the cycle. These involve tephra falls that extend many hundreds of kilometers downwind and local pyroclastic flows that reach beyond 10 km from the vent, especially on the southern flanks. The crater is reamed out to leave an open cylinder (stage 1).

lier historical eruptions described in Luhr and Carmichael (1980, 1990a). These new analyses, which include complete rare earth element (REE) data, are particularly useful in evaluating the relative importance of hornblende and plagioclase fractionation during the 1818–1913 eruptive cycle compared to the 1913–present cycle, a comparison that is central to this study.

2. Historical eruptive cycles of Volcán de Colima

Since Luhr and Carmichael (1980) initially proposed the concept of historical eruptive cycles at Volcán de Colima, three important re-evaluations of the historical eruptive record have been conducted (Medina-Martínez, 1983; De la Cruz-Reyna, 1993; and Bretón et al., 2002–this volume). These investigations pointed out numerous erup-

tions that were not considered by Luhr and Carmichael (1980), and fleshed out observations for many other eruptions. In the light of these studies, and taking account of the frequent eruptions since 1980, the historical eruptive record of Volcán de Colima through 2000 is re-plotted in Fig. 2.

Using the criteria of Newhall and Self (1982), De la Cruz-Reyna (1993) assigned Volcanic Explosivity Index (VEI) values to historical explosive eruptions from Volcán de Colima, including VEI=4 values to large explosive eruptions in 1585, 1606, 1622, 1818, 1890, and 1913 based mainly on reports of the extent of ashfalls. Simkin and Siebert (1994) adopted these six eruptions as VEI=4 (or 4?) in their global compilation. Without referring to the VEI scale, which was published about the same time, Medina-Martínez (1983) equated the magnitudes of three other explosive eruptions in 1590, 1690, and 1806 to those

of 1818 and 1913. For the purposes of this study, all nine of these eruptions are assumed to have been of VEI=4, as plotted on the upper line in Fig. 2.

Of the four most-recent VEI=4 eruptions, those on 15 February 1818 and 20 January 1913 were exceptional, and therefore have been taken by Luhr and Carmichael (1980, 1990a, 1990b) and in this study to mark the transitions in the two most recent eruptive cycles (1818–1913 and 1913–present, Fig. 2), dividing the last half of Volcán de Colima's historical eruptive record into roughly 100-yr parts (Fig. 1, stage 5). Only these two eruptions ejected the lava domes that formerly filled the summit crater, reaming out the crater so that it had the shape of a giant vertical cannon barrel (Fig. 1, stage 1). The dimensions of the crater following the 1818 eruption are in dispute (Bretón et al., 2002-this volume), but the 1913 eruption removed about 100 m from the upper cone and left a crater 450 m in diameter and 350 m deep (Waitz, 1932; Bretón et al., 2002-this volume, figs. 12 and 13). In addition, only the 1818 and 1913 eruptions were followed by ~50-yr intervals during which new lava domes incrementally filled the deep crater but virtually no eruptive activity was

evident outside the crater (Fig. 1, stages 1–2; Fig. 2, stippled fields). From the vantage point of the surroundings, these were non-eruptive years, but lava was erupting, and the crater dome was rising toward the rim. Eventually, block lava from the crater dome began to spill onto the upper flanks (Fig. 1, stage 3).

2.1. 1818–1913

The first lava to erupt external to the crater following the 1818 explosive eruption came in 1869 during an intermittently explosive block-lava eruption from the parasitic vent Volcancito, 1 km NE of the main crater (Fig. 3) (Bretón et al., 2002-this volume, figs. 4–10). At some later point, poorly constrained between 1869 and 1909, another block-lava flow issued from the summit crater and poured down the NW face of the main cone toward the caldera floor (tree-covered double-leveed lava flow at right side of Bretón et al., 2002-this volume, fig. 17). Because the lava descended in this direction, it was completely invisible to observers on the lower flanks of the volcano, and the eruption date may forever remain unknown. Petrographically and compositionally

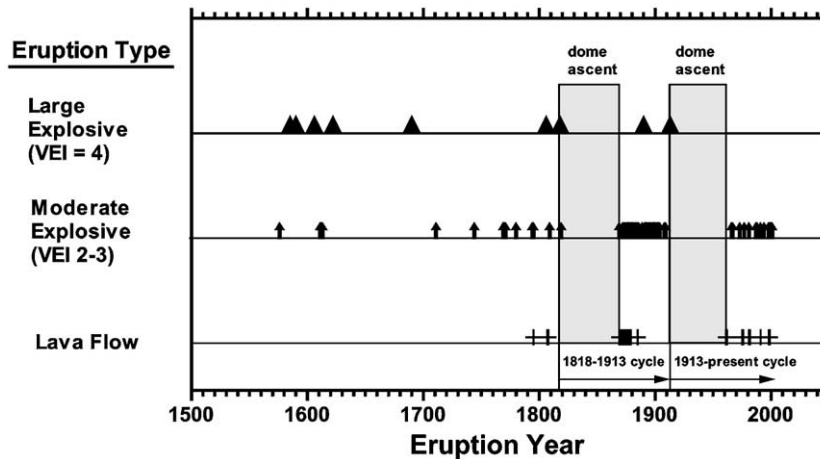


Fig. 2. Historical eruption record of Volcán de Colima, with data from Medina-Martínez (1983), De la Cruz-Reyna (1993), and Bretón et al. (2002-this volume). Eruptions are divided into three types, shown on different horizontal lines: large explosive events similar in magnitude (VEI=4) to those of 1818 and 1913, as judged by at least one of the above authors; moderate explosive eruptions (VEI=2–3); and lava eruptions. Only one eruption of each type is shown for a particular year. Unspecified eruptions are not included. The stippled vertical bars indicate periods of crater-dome ascent following the major explosive eruptions of 1818 and 1913. The 1818–1913 and 1913–present eruptive cycles discussed in Luhr and Carmichael (1980, 1990a) and in this paper are labeled.

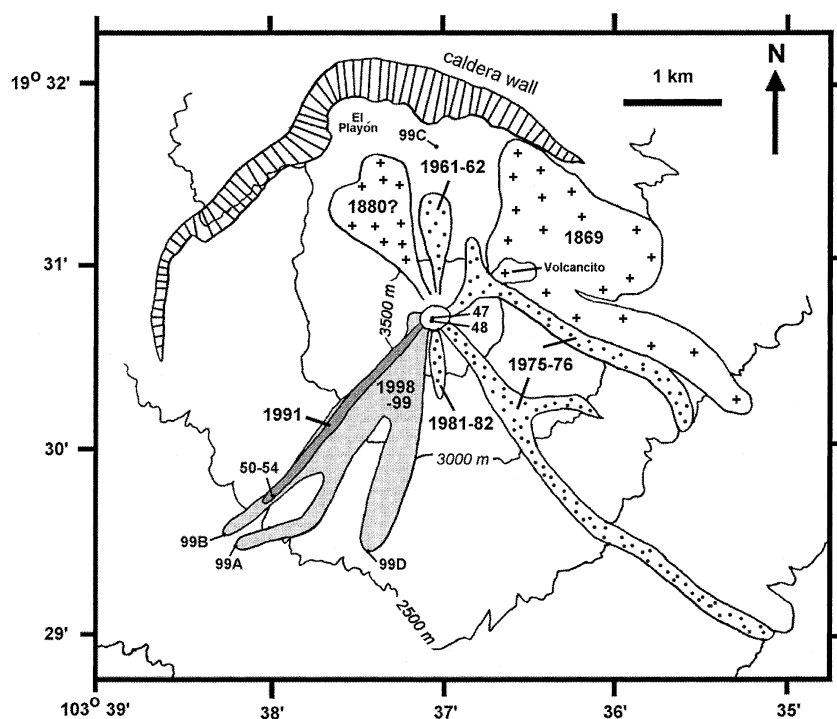


Fig. 3. Sketch map of Volcán de Colima shows the outlines of important lava flows erupted since 1869, including the youngest two lava flows on the SW flank that are the focus of this report: 1991 in dark gray, and 1998–99 in light gray. Small dots indicate the 11 lava samples described in this study. Note that the western 1998–99 lava flow completely buried the 1991 lava flow.

this prominent lava flow is identical to those from Volcancito, so the eruptions were likely close in time. Waitz (1932) implied that this lava flow erupted in 1880, and that date is tentatively adopted in this study (Fig. 2). Numerous small to large explosive eruptions from the summit crater were reported for subsequent years until 1909 (Fig. 1, stage 4; Bretón et al., 2002-this volume, fig. 11). After an apparent 4-yr repose came the major cycle-ending explosive eruption of 1913 (Fig. 1, stage 5).

2.2. 1913–present

The first lava to erupt external to the crater following the 1913 explosive eruption came in 1961 as lava spilled through the low notch in the northern crater rim to feed a small block-lava flow down the north face (Bretón et al., 2002-this volume, fig. 17). Other block-lava flows followed in 1975–1976, 1981–1982, 1991, and

1998–1999 (Fig. 1, stage 3), typically preceded and accompanied by block-and-ash flows that were generated as incandescent lava blocks broke off from the flow margins and crashed down the steep flanks. The extent of these lava flows is shown in Fig. 3. The two most recent eruptions (1991 and 1998–1999) are the focus of this study.

3. 1991 and 1998–99 eruptions and samples studied

3.1. 1991 eruption

In its first magmatic eruption since 1981–82, Volcán de Colima began to extrude a lava dome in the summit crater on 1 March 1991, following increased seismicity, summit deformation, and fumarolic activity during the preceding month (Rodríguez-Elizarrarás et al., 1991). The lava dome fed a block-lava flow, which moved toward the SW crater rim. On 16 April gravitational fail-

ure of the crater rim and the snout of the new lava flow led to the emplacement of block-and-ash flows along the west, central, and east branches of Barranca el Cordoban on the SW flank (Rodríguez-Elizarrarás et al., 1991). Subsequent movement of block lava down the Cordoban west branch was accompanied by continued rockfalls and resultant pyroclastic flows. By 20 April the lava flow was 30 m thick, 300 m long, and 120 m wide; it ultimately reached 3 km in length, extending down to ~2,500 m elevation (Fig. 3) where it was about 20 m thick (Rodríguez-Elizarrarás et al., 1991).

Seven samples were studied from the 1991 eruption. Sample Col-47 was collected in the crater from the new lava dome on 2 March 1991 by Charles B. Connor and Mitch Ventura. Sample Col-48 was collected in the crater from the lava dome on 27 March 1991 by Michael Sheridan. Samples Col-50, -51, -52, -53, and -54 were collected on 13 November 1991, by myself, Julian Flores, and Abel Cortés from the SE levee along the lowermost 100 m of the fully emplaced lava flow about 4 months after the end of its movement (Fig. 3).

3.2. 1998–1999 eruption

The next recognized lava extrusion in Volcán

de Colima's summit crater occurred in late November of 1998, following a summit explosion on 6 July 1998 (Smithsonian Institution, 1998a) and months of precursory ash and thermal emissions (Galindo and Domínguez, 2002-this volume), fumarolic anomalies (Taran et al., 2002-this volume), enhanced seismicity (Reyes-Dávila and De la Cruz-Reyna, 2002-this volume; Zobin et al., 2002a-this volume), and ground-deformation (Murray and Ramirez, 2002-this volume; Ramirez-Ruiz et al., 2002-this volume). At 07.30 h on 20 November 1998, a nearly circular, black lava dome (50×30×15 m) was sighted from a helicopter by geologists from the Colima Volcano Observatory (Navarro-Ochoa et al., 2002-this volume; Zobin et al., 2002b-this volume). Growth of the dome was very rapid and by 11.30 h on 21 November lava began to flow over the SW crater margin, generating block-and-ash flows that extended more than 4 km down the east branch of Barranca el Cordoban (Smithsonian Institution, 1998b). Another flight the same day revealed that the lava flow had advanced ~150 m downslope and had a width of ~100 m and a thickness of ~20 m. Block lava eventually moved down all three branches of Barranca el Cordoban: west, central, and east (Navarro-Ochoa et al., 2002-this volume). The west-branch 1998–1999 lava flow completely buried the 1991 lava

Table 1
Point-counted modes of 1991 and 1998–99 lava samples from Volcán de Colima (vol.%)

Sample: Eruption year:	Col-47 1991	Col-48 1991	Col-50 1991	Col-51 1991	Col-52 1991	Col-53 1991	Col-54 1991	Col-99A 1999	Col-99B 1999	Col-99C 1999	Col-99D 1999
Pl ph	20.5	23.2	25.3	22.4	28.1	28.3	28.2	20.9	24.4	30.3	25.7
Pl mp	2.3	2.4	2.9	4.6	2.9	3.3	3.9	4.1	3.1	3.7	2.1
Cp ph	7.4	6.0	3.6	4.1	2.5	3.5	2.6	4.8	4.1	3.6	4.4
Cp mp	0.9	0.9	0.5	0.8	0.7	0.1	0.5	0.5	0.7	0.4	0.1
Op ph	4.7	5.4	4.5	3.6	5.5	6.7	3.0	4.9	4.3	5.1	3.9
Op mp	2.0	1.7	2.1	3.2	2.2	1.6	2.6	2.0	2.8	3.1	2.2
Hb ph	0.9			0.2	0.2			0.5			
Hb mp									0.1	tr	tr
Ox ph								0.1			
Ox mp	2.0	1.3	2.1	1.4	1.5	0.7	1.3	1.5	1.3	1.3	0.6
Ol xn			0.1			0.4			tr		0.1
Grndm	59.3	59.1	58.9	59.2	56.4	55.4	57.9	60.7	59.3	52.5	61.0

More than 1000 points counted. Abbreviations: ph – phenocryst (>0.3 mm); mp – microphenocryst (>0.03 mm, <0.3 mm: after Wilcox, 1954). Pl – plagioclase; Cp – clinopyroxene; Op – orthopyroxene; Hb – hornblende; Ox – oxide minerals including titanomagnetite and Cr-rich spinel; Ol xn – olivine xenocrysts surrounded by pyroxenes and titanomagnetite; Grndm – ground-mass (<0.03 mm: after Wilcox, 1954).

Table 2
Electron microprobe analyses of pyroxenes and hornblende

Phase:	Opx	Opx	Cpx	Cpx	Hbd1	Hbd2	Hbd
Type:	rims						
Points:	12	10	6	3	2	2	2
Sample:	Col-99A	Col-99B	Col-99A	Col-99B	Col-99A	Col-99A	Col-99B
Mean (wt%)							
SiO ₂	53.18	53.39	50.02	51.10	44.18	41.80	44.97
TiO ₂	0.29	0.28	0.75	0.63	2.25	3.19	1.59
Al ₂ O ₃	1.27	1.36	3.94	2.64	10.39	12.85	10.12
Cr ₂ O ₃	0.01	0.01	0.03	0.01	0.01	0.03	0.07
FeO	16.91	17.21	9.51	9.21	11.87	11.68	12.26
MnO	0.50	0.50	0.26	0.28	0.22	0.14	0.25
MgO	25.64	25.85	14.28	15.04	14.68	13.97	14.96
NiO	0.02	0.01	0.03	0.01	0.01	0.03	0.00
CaO	1.48	1.43	19.80	20.15	10.99	11.04	10.97
Na ₂ O	0.04	0.05	0.55	0.45	2.28	2.62	2.27
K ₂ O	0.02	0.01	0.02	0.02	0.36	0.43	0.30
Cl	n.d.	n.d.	n.d.	n.d.	0.06	0.04	0.07
Total	99.36	100.12	99.19	99.53	97.30	97.82	97.82
1 σ (wt.%)							
SiO ₂	0.29	0.43	0.89	0.13	0.10	0.00	0.81
TiO ₂	0.04	0.03	0.12	0.01	0.05	0.21	0.15
Al ₂ O ₃	0.32	0.48	1.20	0.11	0.22	0.04	0.56
Cr ₂ O ₃	0.01	0.01	0.03	0.01	0.01	0.00	0.02
FeO	0.53	0.45	0.13	0.29	0.02	0.17	0.40
MnO	0.05	0.03	0.04	0.03	0.00	0.02	0.02
MgO	0.34	0.36	0.47	0.19	0.07	0.14	0.50
NiO	0.01	0.01	0.02	0.01	0.01	0.02	0.00
CaO	0.05	0.08	0.37	0.26	0.02	0.10	0.03
Na ₂ O	0.01	0.02	0.05	0.06	0.04	0.01	0.10
K ₂ O	0.01	0.01	0.01	0.01	0.01	0.01	0.00
Cl	n.d.	n.d.	n.d.	n.d.	0.01	0.00	0.00
Mg# (Fe ¹)	73.0	72.8	72.8	74.4	68.8	68.1	68.5
TW (°C)			979	990			
TWB (°C)			966	973			
TBM (°C)			947	953			
TQ (°C)			1047	1029			

Electron microprobe analyses were conducted on the Smithsonian's JEOL-8900 instrument at 15 kV accelerating potential, with a beam current of 20 nA, and a focused spot. Phase: Opx = orthopyroxene, Cpx = clinopyroxene, Hbd = hornblende (two different hornblende crystals in Col-99A yielded distinct analyses, listed as Hbd1 and Hbd2). Type: Rims for pyroxenes gives the mean of analyses taken $\sim 5 \mu\text{m}$ from crystal rims; for hornblende, rims refers to the zone just inside the thin dark reaction rim. Points: The number of spots used to calculate the means. Mg# (Fe¹) = $100 \times \text{Mg}/(\text{Mg} + \text{Fe}^1)$. Equilibration temperatures were calculated from four different pyroxene geothermometers using the mean orthopyroxene and clinopyroxene compositions for the two samples: TW from Wells (1977), TWB from Wood and Banno (1973), TBM from Bertrand and Mercier (1985), and TQ from the QUILF program of Andersen et al. (1993).

flow, which had descended the same barranca. By 7 February 1999, the block-lava flows in the west, central, and east branches of Barranca el Cordoban extended 2.8–3.8 km from the crater rim to elevations of 2400, 2390, and 2560 m, respectively,

and were 20–30 m thick (Smithsonian Institution, 1999a).

Four lava samples were studied from the 1998–1999 eruption (Fig. 3). Sample Col-99D was collected by Ricardo Saucedo on 30 November 1998

from the front of the active block-lava flow in the eastern branch of Barranca el Cordoban. Sample Col-99A was collected by the author, Carlos Navarro, and Mauricio Bretón on 7 February 1999 from the front of the active block-lava flow in the central branch of Barranca el Cordoban (19°29.286'N, 103°38.038'W). Sample Col-99B was collected on the same date by the same team from the front of the active block-lava flow in the western branch of Barranca el Cordoban (19°29.555'N, 103°38.269'W). Sample Col-99C was collected by Francisco Nuñez-Cornú and Carlos Suarez from a 150×80×70-cm ballistic lava bomb in an impact crater on the Playón,

the name given to the caldera floor directly north of the active cone (Fig. 3). It was one of many bombs ejected during an explosion on 10 February 1999 (Smithsonian Institution, 1999a, 1999b). This explosively ejected fragment from the 1999 summit lava dome is thought to provide insight into the magmatic composition at the end of the 1998–1999 eruption.

4. Analytical techniques

Modes were determined by point counting for the 11 lava samples studied from the 1991 and

Table 3
Electron microprobe analyses of plagioclase and groundmass

Phase:	Plag	Plag	Phase:	Grndm	Grndm
Type:	rims	rims	Type:	moving	moving
Points:	10	12	Points:	8	7
Sample:	Col-99A	Col-99B	Sample:	Col-99A	Col-99B
Mean (wt%)			Mean (wt%)		
SiO ₂	55.03	54.70	SiO ₂	66.57	66.31
Al ₂ O ₃	27.99	27.84	TiO ₂	0.58	0.52
Fe ₂ O ₃	0.67	0.71	Al ₂ O ₃	16.13	16.52
CaO	10.65	10.65	FeO	2.39	2.42
Na ₂ O	5.30	5.17	MnO	0.07	0.06
K ₂ O	0.19	0.20	MgO	0.86	1.24
Total	99.84	99.27	CaO	4.39	3.94
			Na ₂ O	5.43	5.48
1σ (wt%)			K ₂ O	2.55	2.26
SiO ₂	0.90	0.88	P ₂ O ₅	0.24	0.19
Al ₂ O ₃	0.50	0.50	Cl	0.10	0.10
Fe ₂ O ₃	0.08	0.11	Total	99.39	99.12
CaO	0.67	0.72			
Na ₂ O	0.34	0.34	1σ (wt%)		
K ₂ O	0.04	0.05	SiO ₂	1.93	2.22
mol% An	52.0	52.6	TiO ₂	0.06	0.15
1σ	3.2	3.3	Al ₂ O ₃	1.16	1.74
			FeO	0.69	0.45
Wt% H ₂ O (Ab)	3.0	3.0	MnO	0.01	0.03
Wt% H ₂ O (An)	3.9	3.8	MgO	0.35	0.66
Wt% H ₂ O (Avg)	3.5	3.4	CaO	1.44	0.81
			Na ₂ O	0.16	0.30
			K ₂ O	0.47	0.33
			P ₂ O ₅	0.07	0.05
			Cl	0.02	0.02

Electron microprobe analyses of plagioclase (Plag) and glassy-to-microcrystalline groundmass (Grndm) were conducted on the Smithsonian's JEOL-8900 instrument at 15 kV accelerating potential, using a beam current of 10 nA, and a 10-μm spot size. The beam was moved by hand during the groundmass analyses. Wt% H₂O (Ab) and (An) are melt water contents predicted by the albite and anorthite exchange algorithms of Housh and Luhr (1991) at the pyroxene temperatures from Table 2 assuming equilibrium between the plagioclase rims and bulk groundmass.

Table 4
Electron microprobe analyses of titanomagnetite, Cr-rich spinel, and olivine

Phase:	Tmt	Tmt	Spinel	Spinel	Spinel	Olivine
Type:	grndm	grndm	oliv. incl.	oliv. incl.	oliv. incl.	xn
Points:	5	6	1	1	1	7
Sample:	Col-99A	Col-99B	Col-99B	Col-99B	Col-99B	Col-99B
Mean (wt%)						
SiO ₂	0.16	0.14	0.08	0.27	0.06	38.67
TiO ₂	10.00	10.22	1.45	0.38	0.38	n.d.
Al ₂ O ₃	2.50	2.56	7.88	6.68	10.29	n.d.
Cr ₂ O ₃	0.28	0.25	17.29	36.36	33.44	n.d.
FeO	78.26	78.30	62.74	46.11	45.33	21.44
MnO	0.46	0.42	0.38	0.45	0.36	0.36
MgO	2.06	2.05	4.57	4.61	6.56	40.08
NiO	0.07	0.05	0.21	0.11	0.17	0.20
CaO	n.d.	n.d.	n.d.	n.d.	n.d.	0.10
Total	93.78	93.99	94.59	94.99	96.61	100.84
1σ (wt%)						
SiO ₂	0.01	0.01				0.40
TiO ₂	0.26	0.20				n.d.
Al ₂ O ₃	0.35	0.35				n.d.
Cr ₂ O ₃	0.11	0.04				n.d.
FeO	0.42	0.53				1.56
MnO	0.03	0.03				0.04
MgO	0.25	0.24				1.39
NiO	0.02	0.03				0.04
CaO	n.d.	n.d.				0.01
Mg# (Fe ^t)						76.9

Electron microprobe analyses were conducted on the Smithsonian's JEOL-8900 instrument at 15 kV accelerating potential, with a beam current of 20 nA, and a focused spot. Phase: Tmt = titanomagnetite. Type: grndm = groundmass, oliv. incl. = Cr-rich spinel inclusion in olivine whose mean composition is also given in this table, xn = xenocryst with pyroxene and titanomagnetite reaction rim. Mg# (Fe^t) as listed in Table 2.

1998–1999 eruptions (Table 1). Mineral and groundmass compositions were also determined for two 1999 lava samples by electron microprobe; pyroxene and hornblende analyses are given in Table 2, plagioclase and groundmass analyses in Table 3, and titanomagnetite, Cr-rich spinel, and olivine analyses in Table 4. Whole-rock powders from the 11 lava samples were analyzed for major elements and 10 trace elements by XRF spectroscopy (Table 5). These same powders were also analyzed for 27 trace elements by ICP-MS along with whole-rock powders for 37 other lava and scoria samples erupted from Volcán de Colima during 1869–1982 and described in Luhr and Carmichael (1980 and 1990a). The ICP-MS data are listed in Table 6. Details of analytical techniques can be found in the footnotes of Tables 1–6.

5. Mineralogy

Samples from the 1991 and 1998–1999 lavas contain the typical phase assemblage of andesites from Volcán de Colima: plagioclase+orthopyroxene+clinopyroxene+titanomagnetite ± hornblende in a groundmass of glass and the same minerals except hornblende. Olivine xenocrysts with Cr-rich spinel inclusions are present in many samples (Table 4), surrounded by reaction coronas of pyroxenes and titanomagnetite (Fig. 4a).

Compositions of phenocryst rims and glassy-to-microcrystalline groundmasses were presented for 16 andesites from Volcán de Colima by Luhr (1992), including three samples erupted in 1991. This study adds complementary data for two lava samples erupted in 1999: Col-99A and Col-99B (Tables 2–4).

Table 5
Major and trace element analyses of whole-rock lavas by XRF spectroscopy

Sample: Eruption year:	Col-47 1991	Col-48 1991	Col-50 1991	Col-51 1991	Col-52 1991	Col-53 1991	Col-54 1991	Col-99A 1999	Col-99B 1999	Col-99C 1999	Col-99D 1999
(wt%)											
SiO ₂	59.33	59.07	59.91	60.14	60.34	59.55	59.12	59.99	60.07	60.39	60.67
TiO ₂	0.67	0.66	0.67	0.67	0.68	0.67	0.66	0.64	0.64	0.62	0.64
Al ₂ O ₃	17.52	17.31	17.61	17.74	17.74	17.46	17.48	17.78	17.79	17.66	17.76
Fe ₂ O ₃	1.79	2.67	1.91	1.77	1.56	1.67	1.66	2.11	1.84	1.99	2.53
FeO	3.81	3.05	3.80	3.89	3.90	3.96	3.93	3.52	3.89	3.51	3.15
MnO	0.11	0.11	0.11	0.11	0.11	0.11	0.11	0.10	0.11	0.10	0.11
MgO	4.00	4.06	3.94	3.89	3.85	3.88	3.91	3.64	3.80	3.50	3.52
CaO	6.35	6.37	6.25	6.33	6.30	6.33	6.29	6.14	6.22	5.98	6.01
Na ₂ O	4.46	4.44	4.51	4.52	4.54	4.46	4.46	4.37	4.36	4.38	4.35
K ₂ O	1.31	1.29	1.31	1.32	1.32	1.28	1.31	1.29	1.30	1.35	1.32
P ₂ O ₅	0.20	0.20	0.20	0.22	0.20	0.20	0.20	0.19	0.20	0.18	0.19
LOI	0.41	0.32	0.33	0.33	0.32	0.32	0.34	−0.01	−0.04	0.00	0.07
Total	99.96	99.55	100.55	100.93	100.86	99.89	99.47	99.76	100.17	99.66	100.32
(ppm)											
V	115	114	120	110	111	118	106	104	109	103	106
Cr	104	98	93	81	73	83	86	75	74	69	71
Ni	39	36	35	35	31	36	33	29	33	29	28
Cu	33	26	28	27	26	26	28	26	25	24	25
Zn	60	58	69	56	56	58	57	57	58	54	57
Rb	18	17	20	19	19	18	18	17	18	19	19
Sr	539	538	542	540	538	539	541	532	532	524	524
Y	17	17	17	17	16	17	18	16	16	16	16
Zr	135	137	139	138	139	136	138	129	128	139	135
Ba	440	459	458	442	448	441	448	442	438	480	464

XRF analyses were performed on the Smithsonian's Philips PW 1480 spectrometer. Major elements were determined on glass disks prepared from 9:1 mixtures of Li-tetraborate and rock powder that had been heated and oxidized during loss on ignition (LOI) determination. Precisions (1σ) were estimated by repeated analysis of one sample and correspond to the following values: SiO₂ = 0.26 wt%, TiO₂ = 0.02%, Al₂O₃ = 0.09%, Fe₂O₃^{Total} = 0.22%, MnO = 0.01%, MgO = 0.08%, CaO = 0.02%, Na₂O = 0.06%, K₂O = 0.04%, and P₂O₅ = 0.01%. FeO was determined by K-dichromate titration following a modified version of the method of Peck (1964). Fe₂O₃ was then calculated from the XRF value for total iron. LOI values are loss on ignition measurements at 1000°C for 1 h on powders dried for several hours at 110°C. These LOI values have not been corrected for oxygen uptake upon conversion of FeO to Fe₂O₃ in the furnace. Trace element analyses by XRF were determined at the Smithsonian on pressed disks made from mixtures of 1.6 g rock powder and 0.4 g cellulose, with a boric acid backing. Precisions (1σ) were estimated by repeated analysis of one sample and correspond to the following percentages of the amounts present: V (19), Cr (5), Ni (4), Cu (8), Zn (2), Rb (3), Sr (1), Y (6), Zr (2), Ba (2).

6. Discussion

6.1. Crystallization conditions

6.1.1. Pyroxene thermometry

Pyroxene phenocryst and microphenocryst rim compositions (Table 2) were used to estimate quench temperatures for these lavas based on two-pyroxene geothermometers (Wood and Banno, 1973; Wells, 1977; Bertrand and Mercier, 1985; Andersen et al., 1993). Large variations

are evident among these estimates for the two samples (100°C and 79°C), although the differences are systematic among the four formulations, with the Bertrand and Mercier (1985) method giving the lowest temperatures and the method of Andersen et al. (1993) the highest. As discussed in Luhr (1992) the experimental study of Brey and Köhler (1990) on lherzolite phase relations showed that for temperatures of concern to this study (900–1000°C) the Wells (1977) formulation closely matched their experimental temperatures,

whereas the Bertrand and Mercier (1985) formulation gave results some 60°C lower. For 18 andesites from Volcán de Colima whose pyroxenes were analyzed in Luhr (1992) and this study (Table 2) the average Wells (1977) temperature is similarly 50°C higher than the average Bertrand and Mercier (1985) temperature. Accordingly we emphasize the Wells (1977) temperatures in the following discussion. Three 1991 samples gave Wells (1977) temperatures of 984–1001°C (Luhr, 1992), and the two 1998–1999 samples listed in Table 2 yielded similar temperatures of 979–990°C.

6.1.2. Experimental analogs

Moore and Carmichael (1998) investigated experimental phase relations for a spessartite (Mas-12) from western Mexico that, except for ~3 wt% higher SiO₂, is compositionally similar to andesites from Volcán de Colima. These results provide important constraints on the temperatures, pressures, and melt water contents of phenocryst crystallization beneath Volcán de Colima. On the T–P_{H₂O} phase diagram for Mas-12 (Fig. 5), the shaded field indicates the stable phenocryst assemblage for hornblende andesites from Volcán de Colima (plagioclase+orthopyroxene+clinopyroxene+hornblende+titanomagnetite), bounded on the low-temperature side by 950°C, the lowest temperature estimated for Colima andesites based on pyroxene thermometry (Wells, 1977). The temperatures estimated for 1991 and 1998–99 hornblende-bearing lavas using this approach lie just above the upper temperature limit for the shaded field of Fig. 5. This discrepancy likely reflects several factors: (1) inherent uncertainties in the pyroxene-based temperatures; (2) the higher silica content of Mas-12 (63.6 wt% SiO₂) compared to andesites from Volcán de Colima (60.3 ± 0.9 wt%); (3) possible water-undersaturated conditions for the Colima magmas, compared to water-saturated conditions in the experiments; and (4) the fact that hornblende is either absent or present in very low amounts in 1991–1999 lavas. The low abundance of hornblende may indicate that these magmas hovered at the upper temperature stability limit of hornblende, which is known to increase with decreasing melt SiO₂

content (Allen and Boettcher, 1978). The phase relations for Mas-12 also indicate that the observed phenocryst assemblage likely grew at pressures between 600 and 1700 bars, equivalent to depths of 2.3–6.6 km beneath the summit of Volcán de Colima, assuming magmatic densities of 2.62 g/cm³. This is the average value of density calculated for 18 andesites from Volcán de Colima based on point-counted modes, estimates of mineral density based on compositional data, and estimates of melt (groundmass) density based on electron-microprobe analyses and partial molar volume data from R. Lange (personal communication, 1999) cited in Luhr (2001). The phase relations of Mas-12 also constrain the melt water contents for hornblende andesites from Volcán de Colima to 3–5 wt% (Fig. 5).

6.1.3. Plagioclase–melt equilibria

Average compositions of plagioclase rims and groundmasses for Col-99A and Col-99B (Table 3) were used to calculate melt water contents at the Wells (1977) temperatures in Table 2 using the Housh and Luhr (1991) model for plagioclase–melt equilibria. Results for the albite and anorthite algorithms (Table 3) yield average values of ~3.5 wt% H₂O, consistent with the phase relations shown in Fig. 5. The compositions of plagioclase rims and glassy-to-microcrystalline groundmasses thus appear to reflect a state of approximate exchange equilibrium prior to degassing, while hornblende was still a stable phase.

6.1.4. Hornblende reaction rims

Hornblende compositions at Volcán de Colima, as determined by electron microprobe, show no systematic differences between scoriae and lavas, but these two products display important differences in hornblende color and texture. Hornblendes in scoriae are pleochroic in green–brown to yellow–brown and show clean contacts against the glassy matrix, whereas hornblendes in block lavas are pleochroic in reddish–brown to yellow–brown and show dark reaction rims against the glassy-to-microcrystalline groundmasses. The color differences reflect higher Fe³⁺/Fe²⁺ in hornblendes from the lavas as a result of oxidation at the surface in contact with the atmosphere.

Table 6
ICP-MS analyses of whole-rock samples from Volcán de Colima (ppm)

Sample	Eruption Year	Sc	Rb	Sr	Y	Zr	Nb	Cs	Ba	La	Ce	Pr	Nd	Sm
1004-410	1869	11.9	21.2	627	15.8	123	3.21	0.68	548	12.5	25.5	3.17	13.5	3.22
1004-412	1869	11.6	21.1	633	15.9	126	3.25	0.68	550	12.5	25.6	3.17	13.6	3.24
Col-2	1869	12.9	20.7	591	15.9		3.22	0.61	519	12.5	25.6	3.22	13.6	3.17
1004-407	1869	12.7	20.8	640	16.5	127	3.30	0.65	543	12.9	26.5	3.30	14.1	3.35
1004-404	1869	13.1	20.7	615	16.5	129	3.36	0.65	530	12.7	26.0	3.24	13.8	3.26
1004-405	1869	13.8	20.3	613	16.6	126	3.33	0.62	532	12.7	26.0	3.26	13.9	3.29
1004-406	1869	12.9	20.6	620	16.4	128	3.37	0.65	537	12.7	26.1	3.27	14.0	3.26
1004-416	1869	12.6	23.5	602	16.6		3.59	0.78	553	13.1	26.8	3.32	14.2	3.29
Col-18	1880	13.9	20.5	602	15.7	119	3.03	0.67	526	11.5	23.3	2.92	12.5	2.99
1004-444	1880	14.4	20.3	606	15.9	119	2.99	0.70	528	11.5	23.7	2.94	12.9	3.18
M82-11	1880	16.9	21.1	602	16.8		3.15	0.63	510	12.1	25.2	3.12	13.4	3.16
M82-10	1880	14.5	20.5	564	17.3	130	3.53	0.66	500	12.5	25.7	3.22	13.9	3.34
1004-443	1880	15.3	21.3	577	16.7		3.12	0.60	497	12.2	25.0	3.17	13.6	3.27
M82-12	1880	13.6	19.4	578	15.5		3.04	0.26	525	11.2	23.7	2.86	12.2	2.95
Col-15	1913	21.5	16.2	596	18.0	116	3.35	0.50	417	11.1	23.3	3.00	13.3	3.41
1004-420	1913	19.3	16.2	592	17.8	117	3.33	0.51	426	11.4	24.0	3.06	13.6	3.41
1004-421	1913	19.9	17.1	604	17.8		3.30	0.49	427	11.4	24.2	3.07	13.6	3.40
1004-415	1913	20.0	16.0	597	17.6	115	3.36	0.48	420	11.2	23.6	3.02	13.4	3.41
98-12A*	1913	19.9	15.3	529	16.4	101	2.80	0.51	433	9.3	19.5	2.51	11.2	2.96
98-12B*	1913	20.6	15.4	521	16.3	101	2.81	0.51	427	9.3	19.3	2.49	11.2	2.93
97-02a*	1913	20.2	17.0	565	17.5		3.27	0.49	424	10.8	22.9	2.90	12.9	3.20
97-02B*	1913	20.1	16.5	559	17.0		3.31	0.50	424	10.6	22.6	2.86	12.6	3.13
97-02C*	1913	20.4	16.8	570	17.1		3.29	0.50	431	10.6	22.6	2.87	12.7	3.17
Col-17.1	1961–62	17.0	22.7	559	18.7		3.62	0.64	503	12.8	26.6	3.32	14.5	3.47
Col-17.2	1961–62	15.1	22.3	544	17.9		3.62	0.65	507	12.8	26.5	3.26	14.2	3.39
Col-17.3	1961–62	15.2	22.9	558	18.0		3.58	0.67	507	13.0	26.5	3.34	14.6	3.36
Col-17.4	1961–62	15.1	21.7	556	17.7		3.51	0.63	502	12.8	26.4	3.25	14.0	3.27
Col-17.5	1961–62	14.8	22.9	567	17.7		3.63	0.65	507	12.7	26.4	3.27	14.0	3.28
Col-17.6	1961–62	15.9	24.3	580	18.1		3.52	0.65	510	13.0	26.6	3.32	14.2	3.39
Col-9	1975–76	14.1	20.0	579	17.1	129	3.52	0.66	498	12.2	25.2	3.11	13.5	3.27
Col-9A	1975–76	14.7	20.1	573	17.4	131	3.51	0.67	498	12.4	25.3	3.14	13.7	3.25
Col-9C	1975–76	14.1	20.7	567	17.3	131	3.53	0.66	501	12.5	25.5	3.14	13.5	3.26
M82-13	1975–76	14.2	20.6	563	17.3	132	3.54	0.67	502	12.4	25.5	3.15	13.6	3.34
Col-40	1976	14.8	19.8	582	17.2	129	3.46	0.65	494	12.2	24.9	3.11	13.4	3.24
M81-13	1976	16.6	18.8	547	16.6		3.50	0.59	462	11.5	23.8	2.94	12.6	3.10
Col-30	1982	19.7	16.7	545	17.0		3.21	0.52	427	10.7	22.3	2.82	12.1	3.11
Col-31	1982	18.4	19.4	561	17.0		3.31	0.51	429	10.6	22.2	2.83	12.3	3.06
Col-47	1991	18.5	21.5	575	16.8		3.46	0.59	462	11.1	23.3	2.92	12.7	3.08
Col-48	1991	18.9	21.3	568	17.4		3.33	0.58	470	11.2	23.4	2.94	12.8	3.19
Col-50	1991	17.5	20.3	561	17.0		3.36	0.65	466	11.4	23.6	2.99	12.8	3.12
Col-51	1991	16.0	18.3	533	16.2		3.28	0.58	470	11.5	24.1	2.99	12.7	3.22
Col-52	1991	16.0	18.1	526	15.7		3.27	0.56	468	11.3	24.0	3.01	12.9	3.13
Col-53	1991	17.6	18.6	547	16.7		3.38	0.59	468	11.3	23.4	2.95	12.6	3.08
Col-54	1991	16.5	18.0	539	16.4		3.34	0.57	463	11.3	23.7	2.99	12.8	3.15
COL99-A	1999	16.4	19.0	552	16.2		3.33	0.59	474	11.5	23.9	2.99	12.9	3.07
COL99-B	1999	17.4	19.0	540	16.4		3.26	0.59	466	11.4	23.7	2.94	12.6	3.12
COL99-C	1999	16.0	20.7	542	16.6		3.46	0.64	495	12.2	25.1	3.09	13.3	3.22
COL99-D	1998	16.1	19.8	548	16.6		3.34	0.61	486	11.7	24.4	3.03	12.9	3.08

Table 6 (Continued).

Sample	Eu	Gd	Tb	Dy	Ho	Er	Tm	Yb	Lu	Hf	Ta	Pb	Th	U
1004-410	1.00	2.92	0.46	2.90	0.59	1.60	0.24	1.53	0.25	3.31	0.23	6.5	1.8	0.70
1004-412	1.02	2.93	0.47	2.84	0.58	1.59	0.24	1.51	0.25	3.31	0.23	6.7	1.8	0.69
Col-2	1.07	3.01	0.49	2.85	0.59	1.61	0.24	1.52	0.25	3.27	0.23	6.0	1.8	0.67
1004-407	1.09	3.00	0.49	2.99	0.62	1.69	0.25	1.57	0.26	3.36	0.24	6.2	1.8	0.67
1004-404	1.02	2.99	0.49	2.88	0.61	1.66	0.24	1.57	0.26	3.34	0.24	6.3	1.9	0.71
1004-405	1.03	3.14	0.49	2.98	0.62	1.72	0.25	1.60	0.26	3.39	0.25	6.4	1.8	0.68
1004-406	1.04	3.06	0.49	2.95	0.61	1.65	0.25	1.60	0.26	3.41	0.24	7.0	1.8	0.68
1004-416	1.07	3.01	0.50	3.05	0.62	1.71	0.25	1.65	0.27	3.39	0.26	7.2	2.0	0.78
Col-18	0.97	2.84	0.46	2.81	0.57	1.55	0.23	1.48	0.25	3.19	0.22	6.3	1.8	0.68
1004-444	1.01	2.91	0.47	2.85	0.59	1.59	0.24	1.54	0.25	3.23	0.23	6.4	1.7	0.66
M82-11	1.06	3.04	0.49	2.96	0.61	1.67	0.25	1.55	0.26	3.17	0.22	7.4	1.7	0.65
M82-10	1.08	3.10	0.51	3.14	0.65	1.78	0.27	1.69	0.28	3.48	0.26	6.3	2.0	0.73
1004-443	1.01	3.04	0.49	2.97	0.60	1.70	0.25	1.56	0.25	3.21	0.22	6.9	1.8	0.67
M82-12	0.95	2.74	0.44	2.70	0.57	1.53	0.23	1.44	0.24	3.12	0.22	4.9	1.7	0.77
Col-15	1.13	3.38	0.54	3.24	0.67	1.84	0.26	1.70	0.26	2.99	0.23	5.2	1.5	0.55
1004-420	1.10	3.21	0.54	3.32	0.66	1.82	0.27	1.68	0.26	3.16	0.24	6.8	1.5	0.57
1004-421	1.14	3.19	0.53	3.16	0.66	1.85	0.27	1.61	0.27	2.99	0.24	4.5	1.5	0.57
1004-415	1.09	3.23	0.54	3.21	0.67	1.81	0.27	1.65	0.27	3.10	0.24	5.3	1.5	0.57
98-12A	0.96	2.87	0.47	2.96	0.62	1.63	0.24	1.57	0.25	2.83	0.20	4.8	1.3	0.51
98-12B	0.95	2.95	0.48	2.95	0.62	1.67	0.25	1.57	0.25	2.83	0.21	4.8	1.4	0.51
97-02a	1.06	3.07	0.53	3.17	0.65	1.79	0.26	1.65	0.26	3.06	0.24	5.4	1.7	0.64
97-02B	1.03	3.00	0.51	3.16	0.65	1.76	0.25	1.65	0.25	3.02	0.23	5.2	1.7	0.66
97-02C	1.08	3.16	0.51	3.08	0.63	1.75	0.25	1.64	0.26	2.99	0.24	6.7	1.8	0.66
Col-17.1	1.10	3.23	0.53	3.24	0.68	1.85	0.26	1.70	0.29	3.50	0.27	6.1	1.9	0.72
Col-17.2	1.05	3.13	0.52	3.17	0.66	1.85	0.27	1.73	0.28	3.47	0.27	6.1	2.0	0.75
Col-17.3	1.06	3.09	0.52	3.13	0.66	1.81	0.27	1.72	0.28	3.56	0.26	6.4	2.0	0.75
Col-17.4	1.07	3.17	0.51	3.10	0.65	1.78	0.27	1.68	0.27	3.48	0.27	6.2	2.0	0.74
Col-17.5	1.03	3.05	0.53	3.13	0.65	1.79	0.27	1.68	0.28	3.46	0.26	6.4	2.0	0.74
Col-17.6	1.08	3.20	0.53	3.15	0.65	1.85	0.27	1.74	0.28	3.55	0.27	6.7	2.0	0.75
Col-9	1.03	3.06	0.50	3.05	0.61	1.73	0.25	1.65	0.27	3.43	0.27	6.4	1.9	0.70
Col-9A	1.02	3.08	0.51	3.02	0.64	1.74	0.26	1.65	0.27	3.37	0.25	6.1	1.9	0.71
Col-9C	1.03	3.12	0.50	2.96	0.62	1.72	0.25	1.66	0.27	3.45	0.26	7.5	1.9	0.70
M82-13	1.03	3.10	0.51	3.05	0.63	1.74	0.26	1.66	0.27	3.49	0.26	6.2	2.0	0.74
Col-40	1.04	3.06	0.50	3.04	0.64	1.70	0.26	1.64	0.27	3.35	0.26	6.2	1.9	0.70
M81-13	1.02	3.08	0.50	3.03	0.63	1.70	0.25	1.59	0.26	3.14	n.d.	5.5	1.7	0.61
Col-30	1.03	3.06	0.51	2.98	0.62	1.67	0.25	1.59	0.25	2.94	0.23	5.1	1.5	0.56
Col-31	1.00	2.87	0.48	2.88	0.61	1.66	0.25	1.56	0.25	3.01	n.d.	5.3	1.6	0.58
Col-47	1.01	2.96	0.48	3.00	0.61	1.69	0.25	1.60	0.26	3.15	0.25	5.8	1.7	0.62
Col-48	1.01	3.02	0.50	2.96	0.62	1.69	0.26	1.62	0.26	3.20	0.24	5.1	1.7	0.63
Col-50	1.03	2.93	0.49	2.99	0.62	1.67	0.25	1.60	0.25	3.19	0.25	5.9	1.7	0.63
Col-51	1.02	3.02	0.50	3.01	0.64	1.71	0.25	1.61	0.26	3.15	0.25	5.9	1.7	0.61
Col-52	1.02	3.12	0.50	3.03	0.63	1.79	0.26	1.65	0.26	3.25	0.25	6.0	1.7	0.63
Col-53	1.01	3.02	0.51	3.09	0.63	1.74	0.25	1.61	0.26	3.14	0.25	5.3	1.7	0.61
Col-54	1.03	3.07	0.50	3.06	0.62	1.72	0.26	1.61	0.26	3.21	0.25	5.3	1.7	0.61
COL99-A	1.02	2.99	0.50	2.97	0.61	1.68	0.26	1.58	0.26	3.24	0.24	5.4	1.7	0.62
COL99-B	1.02	3.00	0.48	2.94	0.60	1.67	0.25	1.56	0.26	3.14	0.25	5.3	1.6	0.62
COL99-C	1.02	3.01	0.50	3.06	0.61	1.74	0.25	1.60	0.26	3.31	0.26	5.3	1.8	0.66
COL99-D	1.01	3.02	0.50	2.99	0.62	1.70	0.25	1.61	0.26	3.26	0.25	5.5	1.7	0.66

ICP-MS analyses were performed at Washington State University (WSU). Estimated 1 σ precisions based on 62 analyses of sample TED run during 1995–1999 correspond to the following percentages of the amounts present: Sc (3.5), Rb (6.7), Sr (1.6), Y (1.7), Nb (4.7), Cs (12.3), Ba (2.5), La (2.3), Ce (1.4), Pr (1.9), Nd (1.5), Sm (2.0), Eu (2.1), Gd (1.5), Tb (1.8), Dy (1.4), Ho (1.4), Er (1.6), Tm (1.8), Yb (1.2), Lu (2.1), Hf (2.4), Ta (9.0), Pb (10.2), Th (7.3), U (9.1). Descriptions of most other samples plus major and trace element data by XRF can be found in Luhr and Carmichael (1980, 1990a). Data for samples from the 1913 eruption marked by asterisks, however, are otherwise unpublished. Missing Zr data indicate samples analyzed prior to March 2000, when WSU added Zr to its analytical routine.

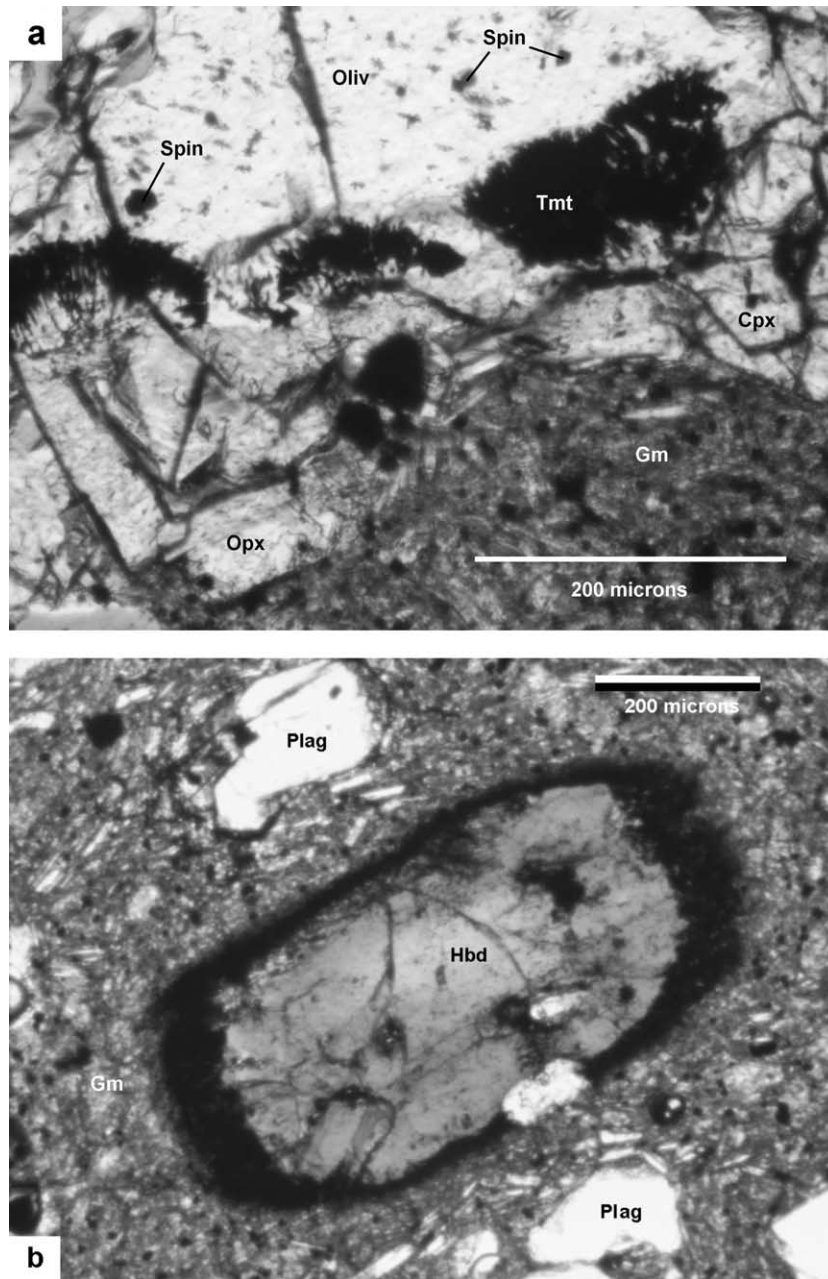


Fig. 4. Photomicrographs in plane light with 200 μm scale bars. (a) Olivine (Oliv) xenocryst with spinel (Spin) inclusions (Table 4) in sample Col-99B separated from the glassy-to-microcrystalline groundmass (Gm) by a reaction corona of orthopyroxene (Opx), clinopyroxene (Cpx), and wormy titanomagnetite (Tmt). (b) Hornblende (Hbd) crystal in sample Col-99A with opacite reaction rim that is thicker ($\sim 75 \mu\text{m}$) in the direction of the prism terminations and thinner ($\sim 20 \mu\text{m}$) in the direction of the prism sides. Two plagioclase (Plag) microphenocrysts and the glassy-to-microcrystalline groundmass (Gm) are also labeled.

The dark hornblende reaction rims in lavas, commonly referred to by the informal name ‘opacite’, have been discussed by many earlier workers and generally attributed to loss of water from the melt, most likely during eruption-related ascent of the magma to pressures below the minimum necessary for hornblende stability (MacGregor, 1938; Kuno, 1950; Jakes and White, 1972; Garcia and Jacobson, 1979). Rutherford and Hill (1993) presented an elegant analysis of this process applied to the 1980–1986 eruptions of Mount St. Helens, in which they combined data on natural samples with results from phase-equilibrium experiments designed to establish the lower pressure limit of hornblende stability and to calibrate rates of amphibole rim growth as magmas pass below that limit during ascent to the surface.

Hornblende is present in seven of the 11 lava samples investigated in this study, in quantities up to 0.9 vol.%. The four samples from the 1998–99 eruption (Col-99A–D) were selected for more rigorous examination of hornblende rim widths, and 6 polished sections were examined for each sample (with a total area of ~ 40 cm²). A total of 86 hornblende rim-width measurements were made in reflected light: 53 for Col-99A, 26 for Col-99B, and only three and four for Col-99C and D, respectively. These abundances mimic point-counted modes in Table 1. As found by Rutherford and Hill (1993) for hornblende reaction rims in Mount St. Helens samples, a considerable range of reaction-rim widths is found in single samples from Volcán de Colima. Islands of anhedral-subhedral hornblende within gabbroic crystal clusters were not considered for the reasons discussed by Rutherford and Hill (1993). The two main types of hornblende rims described by those authors are also present in the andesites from Volcán de Colima: thin (10–50 μ m), black, and fine-grained (<2 μ m), the type referred to as ‘opacite’ in many earlier studies; thicker (up to 1 mm) and coarser grained (20–600 μ m). In contrast with observations in Rutherford and Hill (1993), the thicknesses of thin black rims on many hornblendes from Volcán de Colima are clearly related to crystallographic orientation, with those on *c*-axis prism terminations typically 5 \times thicker than those on prism faces (Fig. 4b). A

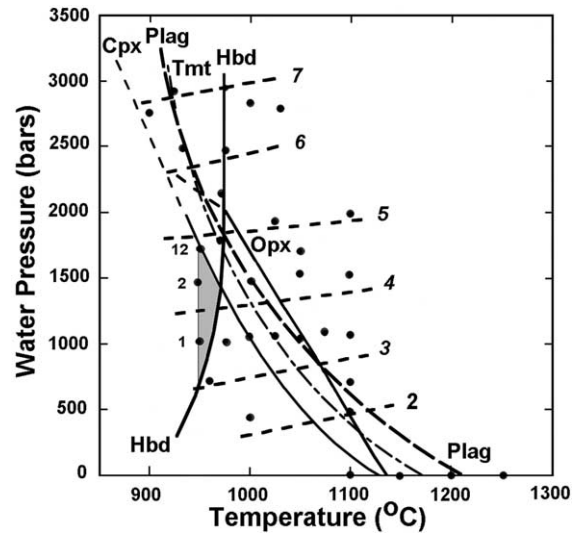


Fig. 5. Water-saturated temperature versus pressure phase relations for Mas-12, a spessartite from the Mascota Volcanic Field that is close in composition to typical andesites from Volcán de Colima (Moore and Carmichael, 1998), although richer in SiO₂: 63.6 wt% normalized anhydrous with all Fe as FeO, versus 60.3 ± 0.9 wt% (1σ) for the 63 andesites erupted from Colima during 1869–1999 and considered in this study. Curves labeled with mineral names indicate first appearance with falling temperature. Dots indicate experimental data points. Gently sloping dashed lines with numerals indicate melt water contents in wt%. The stippled field shows the phenocrystic assemblage for typical hornblende andesites from Volcán de Colima: plagioclase+orthopyroxene+clinopyroxene+hornblende+titanomagnetite. Three experimental points at 950°C and differing $P_{\text{H}_2\text{O}}$ values are labeled with the modal hornblende content (from Moore and Carmichael, 1998), and hint at a strong increase in hornblende abundance with increasing experimental water pressure and melt water content.

histogram of hornblende rim-widths (ignoring prism terminations) shows values from 8 to 65 μ m (Fig. 6); the mode of the population is centered at 20–25 μ m. A few hornblende crystals with much thicker, coarse-grained reaction rims were present but not compiled.

The experimental results of Rutherford and Hill (1993) are thought to be applicable to andesites from Volcán de Colima because the groundmass/glass compositions in both cases are dacitic (Table 3 and Luhr, 1992). However, temperature estimates are 50–100°C higher for Colima andesites and the water-saturated phase diagram of Moore and Carmichael (1998) indicates amphibole stabil-

ity down to ~ 600 bars at 950°C (Fig. 5), ~ 1000 bars lower than the limit determined by Rutherford and Hill (1993).

Rutherford and Hill (1993) interpreted the thin black rims on hornblendes to record crystals that ascended rapidly from the amphibole stability field at a minimum pressure of ~ 1600 bars. They interpreted the thicker, coarser grained rims on other hornblendes to reflect crystals that rose more slowly, likely near the margins of the ascending magma channel. Based on fig. 6 (curve b) of Rutherford and Hill (1993), the most common hornblende reaction rim widths observed in the 1998–1999 lavas from Volcán de Colima (20–25 μm) imply dominant ascent times of 9–11 days since the magmas rose above the hornblende stability field at ~ 1600 bars, equivalent to a depth of 6.3 km, again assuming magmatic densities of 2.62 g/cm^3 . This translates to average magmatic ascent rates of 570–900 m/day. Because most of these samples were collected near the terminations of block-lava flows, ~ 3 km from the vent, some part of these hornblende rims grew during ascent toward the crater, and another part grew during flow of the magma down the thermally insulated lava channel to reach the flow terminus. For those samples the 300–900 m/day ascent rates are minima. Sample Col-99C was potentially very interesting in this regard, since it likely quenched its hornblende-rim growth upon extrusion at the summit, never flowed down the flank, and was blasted from the summit dome on 10 February 1999. Unfortunately only three hornblende crystals were present in the six polished sections from Col-99C; their rim widths of 15, 25, and 38 μm , though far from definitive, hint that little rim growth occurred as the lava flows moved down the flanks.

7. Mineral abundances through time

Much of this study is focused on contrasts between block lavas erupted during 1869–1880 versus block lavas erupted since 1961. Two important mineralogical parameters are shown in Fig. 7 as a function of eruption date: abundances of plagioclase phenocrysts and hornblende pheno-

crysts. The data presented in this study (Table 1) for the 1991 and 1998–1999 eruptions are consistent with the interpretations presented in Luhr and Carmichael (1980, 1990a) based on data for earlier historical eruptions. The 1961–1999 lavas have slightly elevated plagioclase contents compared to lavas erupted in 1869–1880, but the latter are considerably enriched in hornblende. Phase-equilibrium experiments on natural andesitic compositions have demonstrated that increased melt water content preferentially suppresses plagioclase crystallization relative to mafic silicates (Yoder and Tilley, 1962; Sekine et al., 1979; Moore and Carmichael, 1998). Elevated water contents are also necessary to stabilize hornblende in silicate melts. These two effects can be seen on Fig. 5. The three experiments conducted within the hornblende stability field at 950°C show progressively higher hornblende contents (labeled 1, 2, and 12 wt%) with increased melt water contents of 3.5–5.0 wt%, supporting the interpretation that Volcán de Colima's hornblende-rich andesites erupted in 1869–1880 crystallized under considerably higher melt water contents than the hornblende-poor andesites erupted in 1961–1999.

Robin et al. (1991) concurred that Volcán de Colima “displays a pattern of eruptive cyclicality, characterized by lava flows and/or slow effusions in the open crater alternating with short explosive events”. In contrast with the interpretations of this study, however, they regarded the explosively erupted magmas of 1818 and 1913 as the beginnings of eruptive cycles, rather than the ends: in

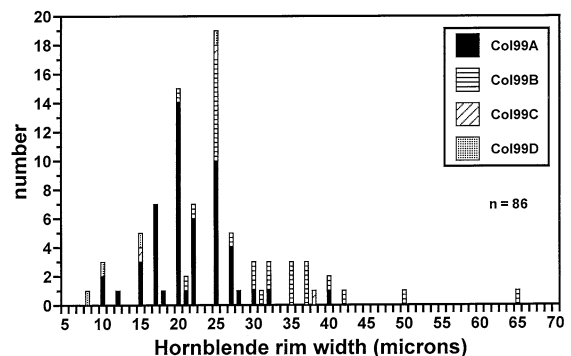


Fig. 6. Histogram of 86 hornblende reaction rim thicknesses in four lava samples erupted in 1998–1999.

their words “the initial mixing stage of a differentiated magmatic body with a new mafic input”. According to the Robin et al. (1991) model, the 1913 mafic andesite was genetically related to the more SiO₂-rich andesitic lavas erupted since 1961. In contrast, according to the model of Luhr and Carmichael (1980 and 1990a) and this study, the 1913 mafic andesite was genetically related to the preceding more SiO₂-rich andesitic lavas erupted in 1869 and 1880. The latter lavas share the hornblende-rich character of the 1913 scoriae, whereas the 1961–1999 lavas do not. This observation supports the interpretation that the explosive eruptions of 1818 and 1913 marked the ends of historical eruptive cycles. According to this view, these eruptive cycles appear to reflect passage of discrete, compositionally zoned magma bodies (upwardly enriched in SiO₂) through the volcanic system on approximately century-long time scales.

8. Whole-rock compositions through time

As discussed in earlier publications (Luhr and Carmichael, 1980, 1990a), Volcán de Colima’s major explosive eruption in 1913 produced scoriae poorer in SiO₂ (58–59%) and richer in MgO (3.5–5.0%) than most of the historical lavas (60–61.5%, 2.5–3.5%) (Fig. 8). On a broader scale, Luhr and Carmichael (1982) showed that scoriae erupted from Volcán de Colima are typically poorer in SiO₂ and richer in MgO compared to block-lava flows. Robin et al. (1991) presented analyses of more silica-rich domains in mingled 1913 scoriae that are compositionally similar to the historical lavas (small inverted triangles on Fig. 8); however, these account for a small fraction of the magma erupted in 1913, and likely represent the remains of the 1869–1880 andesites. Robin et al. (1991) also presented an analysis of a considerably more mafic domain with 56.9 wt% SiO₂ and 7.7% MgO. In contrast, all nine whole-rock scoriae samples from the 1913 deposits that were analyzed for this study fall in the 58–59% SiO₂ range.

The first block-lava flows to leave the summit crater of Volcán de Colima following the vent-clearing 1913 eruption, those erupted in 1961–

1962 and 1975–1976, were fairly homogeneous at ~61 wt% SiO₂ and ~3% MgO (Figs. 8a,b). Beginning with the last dark lobe of lava erupted in 1976, which formed the short flow on the SE flank that reached just past 3000 m (Fig. 3), and continuing through the 1981–1982 lava flow, compositions became decidedly more mafic, with SiO₂ reaching ~58.8% and MgO ~4.5%. These trends appeared to indicate a shift toward mafic magma compositions similar to that erupted explosively in 1913. The data from this study, however, reveal that these compositional trends have since reversed, as seen in the 1991 lava flow and the even more evolved 1998–1999 lavas (Figs. 8a,b). Despite this reversal to less mafic compositions, even the 1998–1999 lavas are still more mafic than all the lavas erupted in 1961–1975, and match closely in composition the last dark lobe of lava erupted in 1976, described above. Temporal patterns similar to that for SiO₂ are evident for Ba (Fig. 8d), La (Fig. 8e), and many other

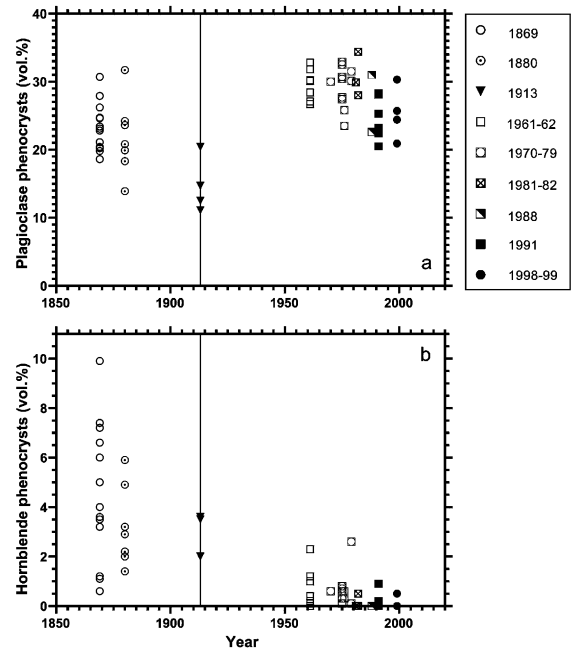


Fig. 7. Eruption year versus modal abundances of phenocrysts (>0.3 mm): (a) plagioclase; (b) hornblende. Compared to the 1869–1913 samples, those erupted in 1961–1999 generally have more plagioclase and significantly less hornblende. Data sources: Luhr and Carmichael (1980, 1990a) and Table 1.

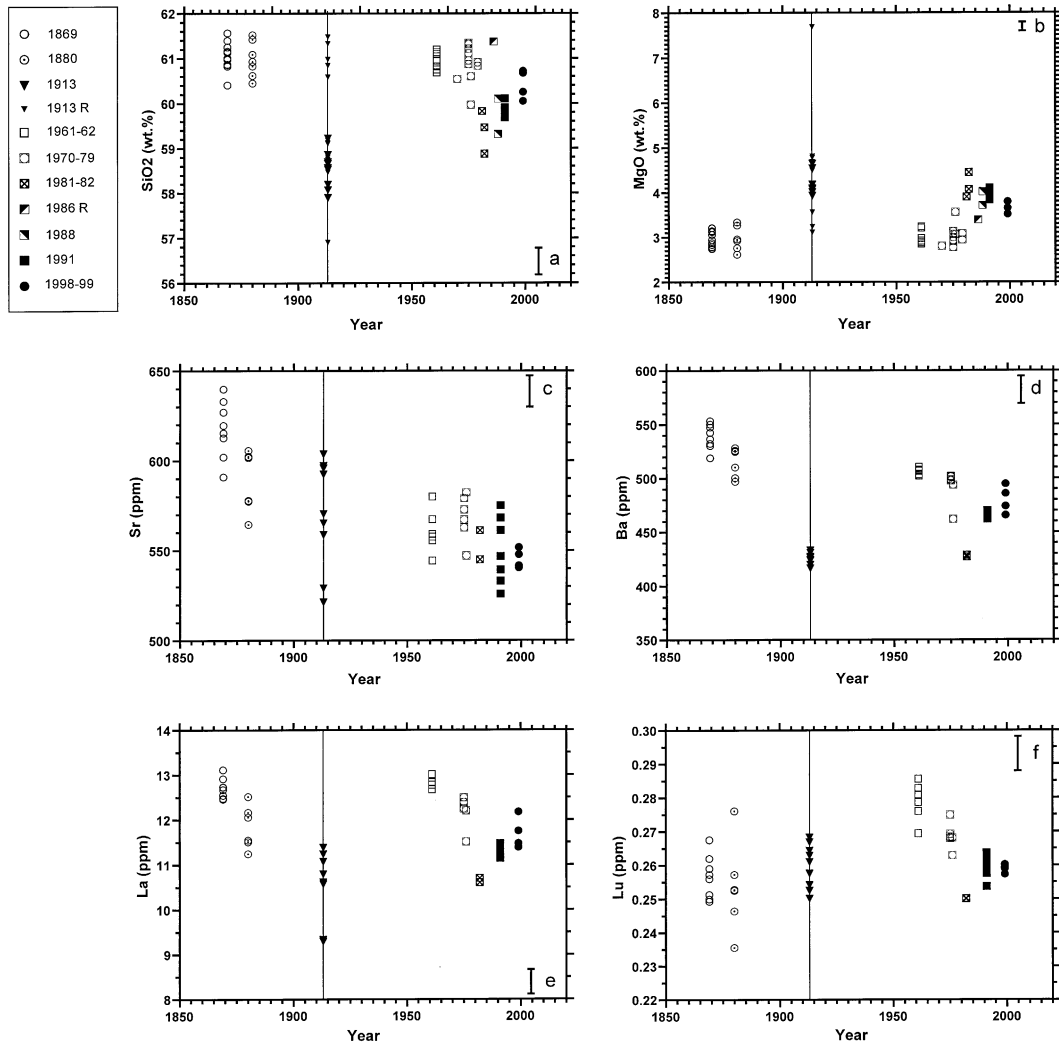


Fig. 8. Eruption year versus whole-rock compositions: (a) SiO₂; (b) MgO; (c) Sr; (d) Ba; (e) La; (f) Lu. Data sources for (a) and (b): 1913 (Luhr and Carmichael, 1980; Luhr and Navarro-Ochoa, unpublished); 1869, 1880, 1961–62, 1970–79, 1981–82, and 1988 (Luhr and Carmichael, 1980, 1990a); 1913 R, and 1986 R (Robin et al., 1991); 1991 and 1998–99, this study (Table 5). Data sources for (c–f): this study (Table 6). SiO₂ and MgO are normalized values after major elements were recalculated to total 100% without loss on ignition and with all iron as FeO. Vertical lines mark the major explosive eruption of 1913. Error bars reflect 1σ analytical precisions (Table 5, SiO₂ and MgO; and Table 6, Sr, Ba, La, and Lu).

incompatible trace elements. Thus, over the period 1976–1999, Volcán de Colima saw a significant mafic excursion that peaked in 1981–1982, but since has been recovering toward the more typical andesites with ~61% SiO₂ that dominated in 1961–1975. Similar fluctuations in the SiO₂ contents of erupted materials, on time scales of years to decades, have been reported at other subduc-

tion-related volcanoes (e.g. Mayon, Philippines (Newhall, 1979); Arenal, Costa Rica (Reagan et al., 1987); Ruapehu, New Zealand (Gamble et al., 1999); and Tongariro, New Zealand (Hobden et al., 1999)), and attributed to periodic recharge of deeper and more mafic magma into a shallower and more differentiated magma reservoir. In the same manner, the upper part of the magma res-

ervoir at Volcán de Colima appears to have been invaded by relatively mafic magma, whose influence was evident in the 1976–1982 lava compositions. If the current eruptive cycle at Volcán de Colima ends with an explosive event similar to that in 1913, involving relatively mafic magma with $\sim 58\%$ SiO_2 , the compositional time series from 1961 to 1999 will certainly not have provided a clear premonitory pattern. Hobden et al. (1999) similarly emphasized the complex temporal trends of Tongariro magma chemistry over the time period 1870–1975, and argued for multiple interactions among small magma batches involving fractional crystallization, magma mixing, and mafic magma recharge.

Pyroxene-rim temperatures using the method of Wells (1977) for the 16 analyzed lava samples erupted in 1869–1999 show a strong negative correlation with whole-rock SiO_2 content (Fig. 9). Pyroxene temperature estimates therefore mirror the SiO_2 trends versus time. The lavas erupted in 1961–1962 and 1975–1976 quenched at 965–980°C according to this algorithm. Temperatures peaked at $\sim 1020^\circ\text{C}$ in the relatively silica-poor lavas of 1981–1982, and have since decreased to 980–995°C in the 1998–99 lavas. Importantly, pyroxene temperatures for two 1913 scoria samples with relatively low SiO_2 contents fall well below the lava regression line. The 1913 scoriae temperatures (970–985°C) overlap those for the preceding 1869–1880 lavas (965–1000°C; Fig. 9). Thus, the entire package of compositionally zoned, hornblende-rich, 1869–1913 magmas was roughly isothermal. The upper part of this system was fairly homogeneously differentiated to phenocryst-rich andesites with $\sim 61\%$ SiO_2 that lost their earlier high water contents prior to erupting as lavas in 1869 and 1880. The lower, more-mafic part of the system, which erupted explosively in 1913, was apparently at a similar temperature, but the magma retained its high water content until eruption, and thus despite lower SiO_2 , had fewer phenocrysts compared to the 1869–1880 lavas (Fig. 7). The high-temperature, low- SiO_2 half of the lava regression (Fig. 9) is entirely defined by lavas erupted in 1982–1999. Importantly, the SiO_2 contents of these lavas overlap those of the explosively erupted 1913 scoriae, but the former record

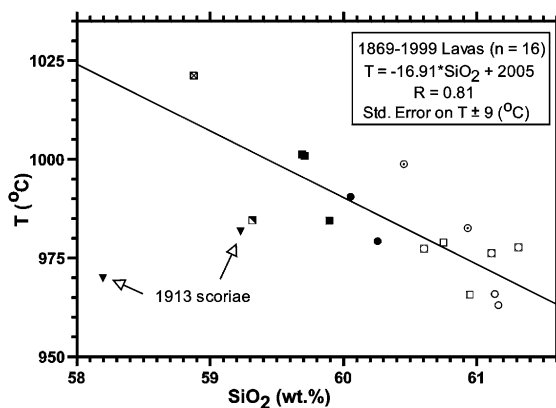


Fig. 9. Temperatures estimated from pyroxene-rim compositions (Wells, 1977) versus whole-rock SiO_2 . Data from Luhr (1992) and Tables 2 and 5. SiO_2 contents normalized as discussed for Fig. 8.

higher temperatures and have higher phenocryst contents. The only explanation for this apparent inconsistency is that the 1982–1999 magmas had considerably lower water contents compared to the 1913 magmas. This independently reinforces the earlier interpretations based on plagioclase and hornblende phenocryst abundances (Fig. 7) that the magmas erupted during 1961–1999 are significantly drier than those erupted during 1869–1913.

During the last two eruptive cycles, the first-erupted lavas showed relative enrichments in many incompatible trace elements compared to later-erupted lavas of similar SiO_2 content (1869 versus 1880, and 1961 versus 1975), although some overlap exists between the two populations. These early enrichments were present in both cases for P_2O_5 , Nb, Ba (Fig. 8d), La (Fig. 8e), Ce, Pr, Nd, Th, and Hf. In addition, the 1869 vs. 1880 samples alone show early enrichments in K and Sr (Fig. 8c), whereas the 1961 vs. 1975 samples show many other early enrichments of Rb, Y, and the middle to heavy REEs Eu, Tb, Dy, Ho, Er, Tm, Yb, and Lu (Fig. 8f). All of the elements enriched in the first lava flows of these two eruptive cycles are relatively incompatible in the phenocrystic assemblage, with the exception of Sr in plagioclase. Presuming that each ~ 100 -yr eruptive cycle involves a discrete compositionally zoned magma body, these trends may indicate

that the uppermost part of the magma body was enriched in melt relative to crystals at some stage.

Table 7 shows a whole-rock compositional comparison of the lavas erupted in 1869–1880 versus those erupted in 1961–1979. The upper limit on the current eruptive cycle was chosen to focus

the comparison on rocks of similar SiO₂ and MgO content, prior to the shift toward more mafic compositions recorded in the 1981–1982 eruption. For elements that are cleanly distinguishable at the 1 σ level between these two groups, the higher values are shown in bold.

Table 7
Comparison of 1869–1880 and 1961–1979 lava compositions

	1869–1880		1961–1979	
	Mean	S.D.	Mean	S.D.
WC and XRF	n = 20		n = 18	
SiO ₂ (wt%)	61.02	0.31	60.91	0.32
TiO ₂	0.64	0.02	0.65	0.03
Al ₂ O ₃	17.95	0.16	17.82	0.21
FeO ⁱ	5.08	0.10	5.27	0.18
MnO	0.10	0.00	0.11	0.01
MgO	3.00	0.22	3.01	0.18
CaO	5.89	0.12	5.97	0.16
Na ₂ O	4.73	0.13	4.68	0.10
K ₂ O	1.40	0.03	1.37	0.03
P ₂ O ₅	0.20	0.01	0.21	0.01
ICP-MS	n = 14		n = 12	
Sc (ppm)	13.6	1.3	15.1	0.9
Rb	20.9	0.9	21.4	1.6
Sr	605	21	565	12
Y	16.3	0.5	17.6	0.5
Zr	125.2	3.6	130.1	1.3
Nb	3.25	0.17	3.55	0.05
Cs	0.63	0.11	0.65	0.02
Ba	528	17	499	12
La	12.3	0.5	12.5	0.4
Ce	25.4	1.0	25.8	0.8
Pr	3.16	0.14	3.20	0.11
Nd	13.5	0.6	13.8	0.5
Sm	3.21	0.11	3.30	0.09
Eu	1.03	0.04	1.05	0.02
Gd	2.98	0.10	3.12	0.06
Tb	0.48	0.02	0.51	0.01
Dy	2.92	0.11	3.09	0.08
Ho	0.60	0.02	0.64	0.02
Er	1.65	0.07	1.77	0.05
Tm	0.25	0.01	0.26	0.01
Yb	1.56	0.06	1.67	0.04
Lu	0.26	0.01	0.27	0.01
Hf	3.30	0.10	3.44	0.11
Ta	0.24	0.01	0.26	0.01
Pb	6.5	0.6	6.3	0.4
Th	1.83	0.07	1.94	0.11
U	0.69	0.04	0.72	0.04

Major elements determined by either wet chemistry (WC) or XRF spectroscopy: Luhr and Carmichael (1980, 1990a). Trace elements determined by ICP-MS from Table 6. Values in bold indicate elements for which the 1 σ ranges of the 1869–1880 and 1961–1979 samples do not overlap; the bolding marks the group with higher concentrations.

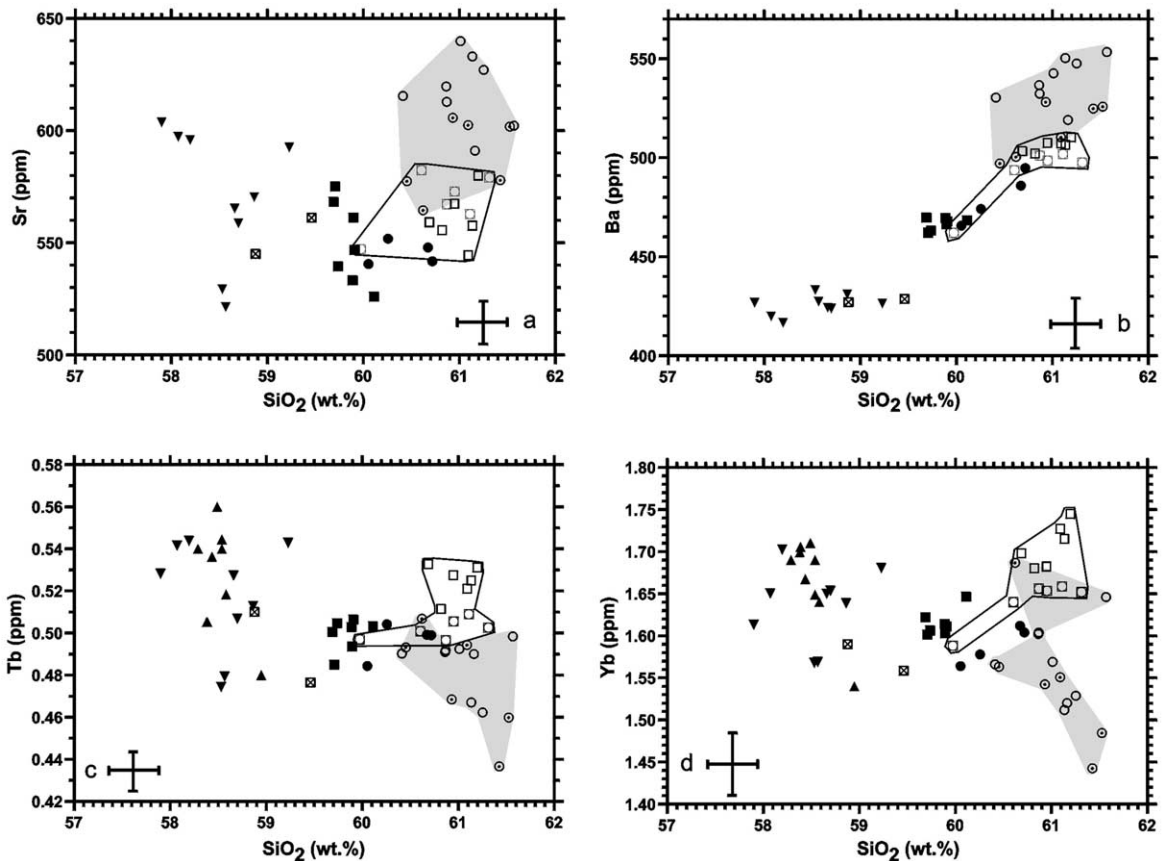


Fig. 10. Whole-rock SiO_2 versus (a) Sr; (b) Ba; (c) Tb; and (d) Yb. Data sources, error bars, and normalization for SiO_2 as discussed for Fig. 8. All trace element values are from Table 6. Stippled fields mark lavas from 1869 and 1880; enclosed fields mark lavas from 1961–1979.

The important differences between these two suites are also seen on time–element plots (Fig. 8) and SiO_2 -variation diagrams (Fig. 10). The lavas erupted in 1869–1880 generally have higher contents of Ba and Sr compared to lavas erupted in 1961–1979 (Table 7; Figs. 8c,d and 10a,b), although again the two populations show some overlap. As shown in Table 8, mineral/melt partition coefficients for Ba and Sr are highest for plagioclase. Thus, these differences are consistent with the inferred higher melt water contents for the 1869–1880 magmas, and consequent relative suppression of plagioclase crystallization. Conversely, Y, Nb, Ta, and the middle to heavy REEs Tb (Fig. 10c), Ho, Er, and Yb (Fig. 10d) are generally enriched in the 1961–1979 lavas compared to those from 1869–1880. A compari-

son of REE patterns for the two suites (Fig. 11) illustrates the middle- to heavy-REE (Gd–Lu) depletions of the 1869–1880 lavas versus the 1961–1979 lavas. Partition coefficients from Table 8 show that these elements are preferentially incorporated into hornblende. Few partition coefficient data are available for Y, Nb, and Ho for the minerals present in andesites from Volcán de Colima, and three closely related elements (Yb, Ta, and Er, respectively) are taken as proxies. Although titanomagnetite has high partition coefficients for Nb and Ta, it is not considered in this analysis because it is a late-stage mineral that is almost entirely restricted to the groundmass. Titanomagnetite is unlikely, therefore, to have affected whole-rock compositions at Volcán de Colima through fractional crystallization.

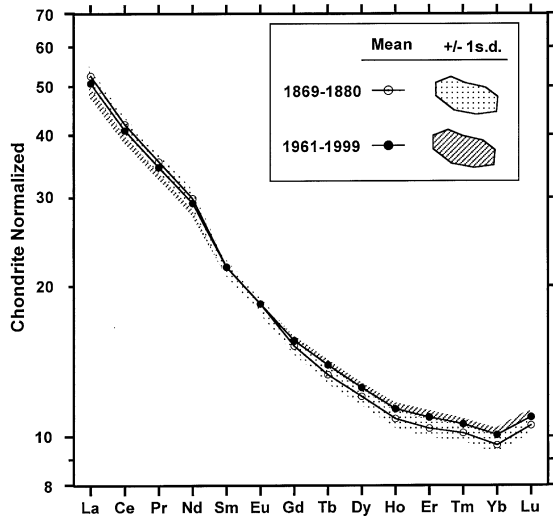


Fig. 11. Chondrite-normalized (relative to C1 chondrite of Anders and Grevesse, 1989) REE diagram contrasts the mean and 1σ values for lavas erupted in 1869–1880 ($n=14$) versus those erupted in 1961–1979 ($n=12$). Note the significant relative depletion of Gd–Lu for the 1869–1880 samples.

In summary, the lavas erupted in 1869–1880 mostly have higher Sr and Ba contents and lower Y, Tb, Ho, Er, Yb, and Ta contents compared to lavas with similar SiO_2 and MgO erupted in 1961–1979. These whole-rock differences are thought to be related to enhanced fractional crystallization of plagioclase in the 1961–1979 magmas, which reduced Sr and Ba in differentiates, and enhanced fractional crystallization of horn-

blende in the 1869–1880 magmas, which reduced Y, Nb, Tb, Ho, Er, Yb, and Ta in differentiates. It is important that the hornblende-rich lavas of 1869–1880 show depletions in hornblende-compatible elements and that the plagioclase-rich lavas of 1961–1979 show depletions in the plagioclase-compatible elements. These observations demonstrate that the whole-rock geochemical differences are opposite those expected from simple crystal accumulation. All evidence is consistent with the interpretation that magmas erupted in 1869–1913 had significantly higher water contents than those erupted in 1961–1999.

9. Conclusions and implications for future eruptive behavior

Will the current eruptive cycle end in a powerful explosive eruption like those that terminated the last two cycles in 1818 and 1913? This is one of the key questions faced by scientists and public officials concerned with Volcán de Colima. Reversing the classic maxim of Hutton, we can assume that ‘the past is the key to the present’ and conclude that the 1818 and 1913 eruptions provide good models for the end of the current cycle. The magmas erupted in 1869–1913 show many subtle but important differences compared with those erupted in 1961–1999, however, all of which are consistent with the interpretation that the lat-

Table 8

Mineral/melt partition coefficients for andesites from the literature

	Hbd	Cpx	Opx	Plag	References
Sr	0.19–0.50	0.06–0.50	0.003–0.13	1.3–5.3	1,2,7,8,9,10
Ba	0.10–0.39	0.02–0.11	0.01–0.23	0.05–0.56	1,2,3,6,7,8,9
La	0.14–0.72	0.05–0.40	0.002–0.30	0.08–0.30	2,3,4,5,6,7,8,10
Sm	1.2–3.0	0.3–1.8	0.03–0.46	0.03–0.11	2,3,4,5,6,7,8,10
Eu	1.2–2.9	0.7–1.6	0.03–0.42	0.36–1.33	2,3,5,6,7,8
Tb	1.5–4.8	1.1–2.7	0.15–0.69	0.05–0.15	2,3,6,7,8
Dy	1.6–4.3	0.8–2.3	0.08–0.56	0.02–0.09	3,4,5,6,8,10
Er	1.5–2.3	0.71	0.15–0.65	0.015–0.045	5,8,10
Yb	1.1–2.3	0.6–2.0	0.25–0.92	0.01–0.04	2,3,4,5,6,7,8,10
Lu	1.0–2.3	0.67–2.0	0.31–1.4	0.01–0.10	2,3,5,6,7,8
Ta	0.56–0.59	0.16–0.50	0.05–0.11	0.03–0.11	6,7,8

References: (1) Philpotts and Schnetzler (1970), (2) Matsui et al. (1977), (3) Luhr and Carmichael (1980), (4) Nicholls and Harris (1980), (5) Fujimaki et al. (1984), (6) Luhr et al. (1984), (7) Bacon and Druitt (1988), (8) Dunn and Sen (1994), (9) Ewart and Griffin (1994), (10) Sisson (1994). Bold highlights mineral with the highest measured partition coefficient. Hbd, hornblende; Cpx, clinopyroxene; Opx, orthopyroxene; Plag, plagioclase.

ter evolved with significantly lower water contents than the former. This fact must be considered in any speculation about eruptive behavior at the termination of the current eruptive cycle. Because expansion of steam derived from magmatic water is the main propellant of explosive volcanism, it is logical to conclude that the termination of the current cycle will involve eruptions less violent than the 1913 event.

Equally important to the original magmatic water content, however, is the extent of magmatic degassing during ascent toward the surface (Woods and Koyaguchi, 1994; Roggensack et al., 1997; Martel et al., 2000). For the relatively mafic andesites that were explosively erupted in 1913 (VEI=4), little pre-eruptive degassing appears to have taken place, as evidenced by a lack of reaction rims on hornblendes with green-brown to yellow-brown pleochroic colors. In contrast, the lavas erupted in 1961–1999 and especially the hornblende-rich lavas erupted in 1869–1880 must have originally had at least 3% H₂O, necessary to stabilize hornblende phenocrysts, but must have lost virtually all of that water prior to reaching the surface. The degassing history of these magmas is elegantly illustrated in a photomicrograph of a hornblende phenocryst with reaction rim from a non-explosively erupted lava sample (Fig. 4b).

Further insight into the termination of the current eruptive cycle at Volcán de Colima demands better understanding of degassing mechanisms beneath the volcano, and the cause of the distinctly different eruptive behaviors for magmas with ~61% SiO₂ compared to those with ~58% SiO₂. This SiO₂ range may mark a critical viscosity and ascent-rate threshold. It appears that magmas erupted from Volcán de Colima with ~58% SiO₂ ascend rapidly through the upper crust without significant degassing, and erupt explosively from the summit crater. In contrast, magmas with SiO₂ contents of ~61% have higher viscosities and appear to rise much more slowly so that they lose most of their volatiles prior to reaching the summit crater and erupting as block-lava flows. This loss of magmatic water at depth undoubtedly helps to feed the persistent vapor plume from the summit of Volcán de Colima.

Acknowledgements

Mauricio Bretón, Charles Connor, Abel Cortés, Julian Flores, Carlos Navarro, Francisco Nuñez-Cornú, Ricardo Saucedo, Michael Sheridan, Carlos Suarez, and Mitch Ventura all assisted in collection of the samples from the 1991 and 1998–1999 eruptions used in this study. I am grateful for both their sweat and their generosity. This work was supported by the Sprague Endowment Fund of the Smithsonian Institution. John Gamble and Mike Garcia provided thorough reviews that led to a major re-thinking of the manuscript. I thank them for helping to make this a better contribution.

References

- Allen, J.C., Boettcher, A.L., 1978. Amphiboles in andesite and basalt: II. Stability as a function of P-T-f_{H2O}-f_{O2}. *Am. Mineral.* 63, 1074–1087.
- Anders, E., Grevesse, N., 1989. Abundances of the elements: meteoritic and solar. *Geochim. Cosmochim. Acta* 53, 197–214.
- Andersen, D.J., Lindsley, D.H., Davidson, P.M., 1993. QUILF: A PASCAL program to assess equilibria among the Fe-Mg-Mn-Ti oxides, pyroxenes, olivine, and quartz. *Comp. Geosci.* 19, 1333–1350.
- Bacon, C.R., Druitt, T.H., 1988. Compositional evolution of the zoned calcalkaline magma chamber of Mount Mazama, Crater Lake, Oregon. *Contrib. Mineral. Petrol.* 98, 224–256.
- Bertrand, P., Mercier, J.-C.C., 1985. The mutual solubility of coexisting ortho- and clinopyroxene: toward an absolute geothermometer for the natural system? *Earth Planet. Sci. Lett.* 76, 109–122.
- Bretón, M., Ramírez, J.J., Navarro, C., 2002. Summary of the historical eruptive activity of Volcán de Colima, México: 1519–2000. *J. Volcanol. Geotherm. Res.* 117, 21–46.
- Brey, G.P., Köhler, T., 1990. Geothermometry in four-phase lherzolites II. New thermobarometers, and practical assessment of existing thermobarometers. *J. Petrol.* 31, 1353–1378.
- Camus, G., Gourgaud, A., Vincent, P.M., 1987. Petrologic evolution of Krakatau (Indonesia): implications for a future activity. *J. Volcanol. Geotherm. Res.* 33, 299–316.
- Cashman, K.V., 1988. Crystallization of Mount St. Helens 1980–1986 dacite: A quantitative textural approach. *Bull. Volcanol.* 50, 194–209.
- Cashman, K.V., 1992. Groundmass crystallization of Mount St. Helens dacite, 1980–1986: A tool for interpreting shallow magmatic processes. *Contrib. Mineral. Petrol.* 109, 431–449.
- Cashman, K.V., Taggart, J.E., 1983. Petrologic monitoring of

- 1981 and 1982 eruptive products from Mount St. Helens. *Science* 221, 1385–1387.
- Corsaro, R.A., Cristofolini, R., 1996. Origin and differentiation of recent basaltic magmas from Mount Etna. *Mineral. Petrol.* 57, 1–21.
- De la Cruz-Reyna, S., 1993. Random patterns of activity at Colima Volcano, México. *J. Volcanol. Geotherm. Res.* 55, 51–68.
- Dunn, T., Sen, C., 1994. Mineral/matrix partition coefficients for orthopyroxene, plagioclase, and olivine in basaltic to andesitic systems: A combined analytical and experimental study. *Geochim. Cosmochim. Acta* 58, 717–733.
- Ewart, A., Griffin, W.L., 1994. Application of proton-microprobe data to trace-element partitioning in volcanic rocks. *Chem. Geol.* 117, 251–284.
- Fedotov, S.A., Balesta, S.T., Dvigalo, V.N., Razina, A.A., Flerov, G.B., Chirkov, A.M., 1991. New Tolbachik volcanoes. In: Fedotov, S.A., Masurenkov, Yu.P. (Eds.), *Active Volcanoes of Kamchatka, Vol. 1*. Nauka Publishers, Moscow, pp. 275–279.
- Fujimaki, H., Tatsumoto, M., Aoki, K.-I., 1984. Partition coefficients of Hf, Zr, and REE between phenocrysts and groundmass. *J. Geophys. Res.* 89 (Suppl.), B662–B772.
- Galindo, I., Domínguez, T., 2002. Near real-time satellite monitoring during the 1997–2000 activity of Volcán de Colima (México) and its relationship with seismic monitoring. *J. Volcanol. Geotherm. Res.* 117, 91–104.
- Gamble, J.A., Wood, C.P., Price, R.C., Smith, I.E.M., Stewart, R.B., Waight, T., 1999. A fifty year perspective of magmatic evolution on Ruapehu Volcano, New Zealand: Verification of open system behaviour in an arc volcano. *Earth Planet. Sci. Lett.* 170, 301–314.
- Garcia, M.O., Jacobson, S.S., 1979. Crystal clots, amphibole fractionation, and the evolution of calc-alkaline magmas. *Contrib. Mineral. Petrol.* 69, 319–332.
- Geschwind, C.H., Rutherford, M.J., 1995. Crystallization of microlites during magma ascent: The fluid mechanics of 1980–1986 eruptions at Mount St. Helens. *Bull. Volcanol.* 57, 356–370.
- Harris, D.M., Anderson, A.T., 1983. Concentrations, sources, and losses of H₂O, CO₂, and S in Kilauean basalt. *Geochim. Cosmochim. Acta* 47, 1139–1150.
- Hobden, B.J., Houghton, B.F., Davidson, J.P., Weaver, S.D., 1999. Small and short-lived magma batches at composite volcanoes: Time windows at Tongariro volcano, New Zealand. *J. Geol. Soc. London* 156, 865–868.
- Housh, T.B., Luhr, J.F., 1991. Plagioclase-melt equilibria in hydrous systems. *Am. Mineral.* 76, 477–492.
- Ihinger, P.D., Hervig, R.L., McMillan, P.F., 1994. Analytical methods for volatiles in glasses. In: Carroll M.R., Holloway, J.R. (Eds.), *Volatiles in Magmas*. Mineral. Soc. Am. Rev. Mineral. 30, 67–121.
- Jakes, P., White, A.J.H., 1972. Hornblendes from calc-alkaline volcanic rocks of island arcs and continental margins. *Am. Mineral.* 57, 887–902.
- Kuno, H., 1950. Petrology of Hakone Volcano and adjacent areas, Japan. *Geol. Soc. Am. Bull.* 61, 957–1020.
- Luhr, J.F., 1992. Slab-derived fluids and partial melting in subduction zones: Insights from two contrasting Mexican volcanoes (Colima and Ceboruco). *J. Volcanol. Geotherm. Res.* 54, 1–18.
- Luhr, J.F., 2001. Glass inclusions and melt volatile contents at Parícutin Volcano, México. *Contrib. Mineral. Petrol.* 142, 261–283.
- Luhr, J.F., Carmichael, I.S.E., 1980. The Colima Volcanic Complex, México: Part I. Post-caldera andesites from Volcán Colima. *Contrib. Mineral. Petrol.* 71, 343–372.
- Luhr, J.F., Carmichael, I.S.E., 1982. The Colima Volcanic Complex, México: Part III. Ash- and scoria-fall deposits from the upper slopes of Volcán Colima. *Contrib. Mineral. Petrol.* 80, 262–275.
- Luhr, J.F., Carmichael, I.S.E., 1990a. Petrological monitoring of cyclical eruptive activity at Volcán Colima, México. *J. Volcanol. Geotherm. Res.* 42, 235–260.
- Luhr, J.F., Carmichael, I.S.E., 1990b. Geology of Volcán de Colima. *Univ. Nac. Auton. México, Inst. Geol. Bol.* 107, 101 pp.
- Luhr, J.F., Carmichael, I.S.E., Varekamp, J.C., 1984. The 1982 eruptions of El Chichón Volcano, Chiapas, México: Mineralogy and petrology of the anhydrite-bearing pumices. *J. Volcanol. Geotherm. Res.* 23, 69–108.
- MacGregor, A.G., 1938. The volcanic history and petrology of Montserrat, with observations on Mt. Pelee in Martinique. *Philos. Trans. R. Soc. London Ser.* 229, 1–90.
- Martel, C., Bourdier, J.-L., Pichavant, M., Traineau, H., 2000. Textures, water content and degassing of silicic andesites from recent plinian and dome-forming eruptions at Mount Pelée volcano (Martinique, Lesser Antilles arc). *J. Volcanol. Geotherm. Res.* 96, 191–206.
- Matsui, Y., Onuma, N., Nagasawa, H., Higuchi, H., Banno, S., 1977. Crystal structure control in trace element partition between crystal and magma. *Bull. Soc. Fr. Mineral. Cristallogr.* 100, 315–324.
- McBirney, A.R., Taylor, H.P., Jr., Armstrong, R.L., 1987. Parícutin re-examined: A classic example of crustal assimilation in calc-alkaline magma. *Contrib. Mineral. Petrol.* 95, 4–20.
- Medina-Martínez, F., 1983. Analysis of the eruptive history of the Volcán de Colima, México (1560–1980). *Geofis. Int.* 22, 157–178.
- Melson, W.G., 1983. Monitoring the 1980–1982 eruptions of Mount St. Helens: Compositions and abundances of glass. *Science* 221, 1387–1391.
- Métrich, N., Clocchiatti, R., 1989. Melt inclusion investigation of the volatile behavior in historic alkaline magmas of Etna. *Bull. Volcanol.* 51, 185–198.
- Métrich, N., Clocchiatti, R., Moshbah, M., Chaussidon, M., 1993. The 1989–1990 activity of Etna: Magma mingling and ascent of H₂O-Cl-S-rich basaltic magma. Evidence from melt inclusions. *J. Volcanol. Geotherm. Res.* 59, 131–144.
- Moore, G.M., Carmichael, I.S.E., 1998. The hydrous phase equilibria (to 3 kbar) of an andesite and basaltic andesite from western Mexico: Constraints on water content and

- conditions of phenocryst growth. *Contrib. Mineral. Petrol.* 130, 304–319.
- Murray, J.B., Ramírez Ruiz, J.J., 2002. Long-term predictions of the time of eruptions using remote distance measurement at Volcán de Colima, México. *J. Volcanol. Geotherm. Res.* 117, 79–89.
- Navarro-Ochoa, C., Gavilanes, J.C., Cortés, A., 2002. Movement and emplacement of lava flows at Volcán de Colima, México: Nov. 1998–Feb. 1999. *J. Volcanol. Geotherm. Res.* 117, 155–167.
- Newhall, C.G., 1979. Temporal variation in the lavas of Mayon volcano, Philippines. *J. Volcanol. Geotherm. Res.* 6, 61–83.
- Newhall, C.G., Self, S., 1982. The volcanic explosivity index (VEI): An estimate of explosive magnitude for historical volcanism. *J. Geophys. Res.* 87, 1231–1238.
- Nicholls, I.A., Harris, K.L., 1980. Experimental rare earth element partition coefficients for garnet, clinopyroxene, and amphibole coexisting with andesitic and basaltic liquids. *Geochim. Cosmochim. Acta* 44, 287–308.
- Pallister, J.S., Hoblitt, R.P., Crandell, D.R., Mullineaux, D.R., 1992. Mount St. Helens a decade after the 1980 eruptions: Magmatic models, chemical cycles, and a revised hazards assessment. *Bull. Volcanol.* 54, 126–146.
- Pallister, J.S., Hoblitt, R.P., Meeker, G.P., Knight, R.J., Siems, D.F., 1996. Magma mixing at Mount Pinatubo: Petrographic and chemical evidence from the 1991 deposits. In: Newhall, C.G., Punongbayan, R.S. (Eds.), *Fire and Mud: Eruptions and Lahars of Mount Pinatubo*, Philippines, Philippine Institute of Volcanology and Seismology, Quezon City, and University of Washington Press, Seattle, WA, pp. 687–731.
- Peck, L.C., 1964. Systematic analysis of silicates. *U.S. Geol. Surv. Bull.* 1170, 89 pp.
- Philpotts, J.A., Schnetzler, C.C., 1970. Phenocryst-matrix partition coefficients for K, Rb, Sr, and Ba, with applications to anorthosite and basalt genesis. *Geochim. Cosmochim. Acta* 36, 1131–1166.
- Pietruszka, A.J., Garcia, M.O., 1999. A rapid fluctuation in the mantle source and melting history of Kilauea volcano inferred from the geochemistry of its historical summit lavas (1790–1982). *J. Petrol.* 40, 1321–1342.
- Ramírez Ruiz, J.J., Santiago-Jimenez, H., Alatorre-Chavez, E., Bretón-Gonzalez, M., 2002. EDM deformation monitoring of the 1997–2000 eruption at Volcán de Colima. *J. Volcanol. Geotherm. Res.* 117, 61–67.
- Reagan, M.K., Gill, J.B., Malavassi, E., Garcia, M.O., 1987. Changes in magma composition at Arenal Volcano, Costa Rica, 1968–1985: Real-time monitoring of open-system differentiation. *Bull. Volcanol.* 49, 415–434.
- Reyes-Dávila, G.A., De la Cruz-Reyna, S., 2002. Experience in the short-term eruption forecasting at Volcán de Colima, Mexico, and public response to forecasts. *J. Volcanol. Geotherm. Res.* 117, 121–127.
- Robin, C., Camus, G., Gourgaud, A., 1991. Eruptive and magmatic cycles at Fuego de Colima volcano (Mexico). *J. Volcanol. Geotherm. Res.* 45, 209–225.
- Rodríguez-Elizarrarás, S., Siebe, C., Komorowski, J.-C., Espíndola, J.M., Saucedo, R., 1991. Field observations of pristine block- and ash-flow deposits emplaced April 16–17, 1991 at Volcán de Colima, Mexico. *J. Volcanol. Geotherm. Res.* 48, 399–412.
- Roggensack, K., Hervig, R.L., McKnight, S.B., Williams, S.N., 1997. Explosive basaltic volcanism from Cerro Negro volcano: Influence of volatiles on eruptive style. *Science* 277, 1639–1642.
- Rutherford, M.J., Devine, J.D., 1998. Changing magma conditions and ascent rates during the Soufriere Hills eruption on Montserrat. *Geol. Soc. Am. Today* 8, 1–7.
- Rutherford, M.J., Hill, P.M., 1993. Magma ascent rates from amphibole breakdown: An experimental study applied to the 1980–1986 Mount St. Helens eruptions. *J. Geophys. Res.* 98, 19667–19685.
- Scarpa, R., Tilling, R.I. (Eds.), 1996. *Monitoring and Mitigation of Volcano Hazards*. Springer, Berlin, 841 pp.
- Sekine, T., Katsura, T., Aramaki, S., 1979. Water saturated phase relations of some andesites with application to estimation of the initial temperature and water pressure at the time of eruption. *Geochim. Cosmochim. Acta* 43, 1367–1376.
- Simkin, T., Siebert, L., 1994. *Volcanoes of the World*, 2nd edn. Geoscience Press, Phoenix, AZ, 349 pp.
- Sisson, T.W., 1994. Hornblende-melt trace-element partitioning as measured by ion microprobe. *Chem. Geol.* 117, 331–344.
- Smithsonian Institution, 1998. Colima. *Bull. Glob. Volcanism Netw.*, Smithsonian Institution, Washington, DC, 23, 10.
- Smithsonian Institution, 1998. Colima. *Bull. Glob. Volcanism Netw.*, Smithsonian Institution, Washington, DC, 23, 11.
- Smithsonian Institution, 1999a. Colima. *Bull. Glob. Volcanism Netw.*, Smithsonian Institution, Washington, DC, 24, 1.
- Smithsonian Institution, 1999b. Colima. *Bull. Glob. Volcanism Netw.*, Smithsonian Institution, Washington, DC, 24, 2.
- Taran, Y., Gavilanes-Ruiz, J.C., Cortés, A., 2002. Chemical and isotopic composition of fumarolic gases and the SO₂ flux from Volcán de Colima, México, between 1994 and 1998 eruptions. *J. Volcanol. Geotherm. Res.* 117, 105–119.
- Waitz, P., 1932. Datos historicos y bibliographicos acerca del Volcán de Colima. *Mem. Rev. Soc. Cient. Antonio Alzate, Mexico* 53, 349–384.
- Wells, P.R.A., 1977. Pyroxene thermometry in simple and complex systems. *Contrib. Mineral. Petrol.* 62, 129–139.
- Wilcox, R.E., 1954. Petrology of Parícutin Volcano, México. *US Geol. Surv. Bull.* 965C, 281–353.
- Wood, B.J., Banno, S., 1973. Garnet-orthopyroxene and orthopyroxene-clinopyroxene relationships in simple and complex systems. *Contrib. Mineral. Petrol.* 42, 109–124.
- Woods, A.W., Koyaguchi, T., 1994. Transitions between explosive and effusive eruptions of silicic magmas. *Nature* 370, 641–644.
- Yoder, H.S., Jr., Tilley, C.E., 1962. Origin of basaltic magmas: An experimental study of natural and synthetic rock systems. *J. Petrol.* 3, 342–532.

Zobin, V.M., González-Amescua, M., Reyes-Dávila, G.A., Domínguez, T., Cerda-Chacón, J.C., Chávez-Álvarez, J.M., 2002a. Comparative characteristics of the 1997–1998 seismic swarms preceding the November 1998 eruption of Volcán de Colima, Mexico. *J. Volcanol. Geotherm. Res.* 117, 47–60.

Zobin, V.M., Luhr, J.F., Taran, Y.A., Bretón, M., Cortés, A., De La Cruz-Reyna, S., Domínguez, T., Galindo, I., Gavi-lanes, J.C., Muñiz, J.J., Navarro, C., Ramírez, J.J., Reyes, G.A., Ursúa, M., Velasco, J., Alatorre, E., Santiago, H., 2002b. Overview of the 1997–2000 activity of Volcán de Colima, México. *J. Volcanol. Geotherm. Res.* 117, 1–19.